Review Article

Kenya Kandwal[#], Alok Jain, Rajeev Kumar*, Shubham Sharma*[#], Pardeep Singh Bains, Ashish Sharma, Sanjeev Kumar Joshi, Dražan Kozak, Mohamed Abbas, and Jasmina Lozanovic

Critical review on the derivative of graphene with binary metal oxide-based nanocomposites for high-performance supercapacitor electrodes

https://doi.org/10.1515/mgmc-2023-0027 received October 18, 2023; accepted July 11, 2024

Abstract: Supercapacitors, owing to their high power density and rapid charge—discharge capabilities, have gained

Shubham Sharma has participated equally in the manuscript so he should be considered as Co-first author.

Kenya Kandwal: Research Scholar, School of Chemical Engineering and Physical Sciences, Lovely Professional University, Jalandhar, 144411, Punjab, India **Alok Jain:** School of School of Chemical Engineering and Physical Sciences, Lovely Professional University, Jalandhar, 144411, Punjab, India, e-mail: alok.jain@lpu.co.in

Pardeep Singh Bains: Department of Mechanical Engineering, Faculty of Engineering and Technology, Jain (Deemed-to-be) University, Bengaluru, Karnataka, 560069, India; Department of Mechanical Engineering, Vivekananda Global University, Jaipur, Rajasthan, 303012, India Ashish Sharma: School of Mechanical Engineering, Lovely Professional University, Jalandhar, 144411, Punjab, India, e-mail: Ashish.16420@lpu.co.in Sanjeev Kumar Joshi: Department of Mechanical Engineering, Uttaranchal Institute of Technology, Uttaranchal University, Dehradun, 248007, India, e-mail: ersanjeevjoshi@gmail.com

Dražan Kozak: Department of Mechanical Engineering, University of Slavonski Brod, Mechanical Engineering Faculty in Slavonski Brod, Trg Ivane Brlić-Mažuranić 2, HR-35000 Slavonski Brod, Croatia, e-mail: dkozak@unisb.hr

Mohamed Abbas: Electrical Engineering Department, College of Engineering, King Khalid University, Abha 61421, Saudi Arabia, e-mail: mabas@kku.edu.sa

Jasmina Lozanovic: Department of Engineering, University of Applied Sciences Campus Vienna, 1100, Vienna, Austria, e-mail: jasmina.lozanovic@fh-campuswien.ac.at

significant attention as energy storage devices in various applications. In the context of electrochemical supercapacitors, this article provides a comprehensive review of the production and electrochemical performance of binary metal oxide (BMO) and reduced graphene oxide (rGO) composite materials. The synthesis processes and synergistic benefits of BMO-rGO composites, with an emphasis on how they perform better than separate parts in terms of specific capacitance and cycle stability, are discussed. The potential of BMO-rGO composites as high-performance electrode materials for supercapacitors is highlighted in this research. In the context of electrochemical supercapacitors, this work provides a comprehensive review of the production and electrochemical performance of binary transition metal oxide (TMO) and rGO composite materials. Composite materials with enhanced electrochemical characteristics that are appropriate for supercapacitor applications are the primary novelty, which is the synergistic combination of rGO with a variety of TMOs. Compared to individual TMOs or other carbonaceous materials, these composites demonstrate enhanced specific capacitance, energy density, power density, cyclic stability, and rate capability. The synthesis processes and synergistic benefits of BMO-rGO composites are discussed, with an emphasis on their superior performance in specific capacitance and cycle stability compared to individual components. This research highlights the potential of BMO-rGO composites as high-performance electrode materials for supercapacitors, showcasing their enhanced specific capacitance, improved charge storage capacity, increased power density, excellent cycling stability, and overall durability even after numerous charge-discharge cycles.

Keywords: binary transition, supercapacitor, graphene, rGO, graphene oxide

Acronyms and abbreviations

A·g⁻¹ Ampere per gram
ASCs Asymmetrical supercapacitors

^{*} Corresponding author: Rajeev Kumar, School of Mechanical Engineering, Lovely Professional University, Jalandhar, 144411, Punjab, India, e-mail: Rajeev.14584@lpu.co.in

^{*} Corresponding author: Shubham Sharma, Centre of Research Impact and Outcome, Chitkara University Institute of Engineering and Technology, Chitkara University, Rajpura, 140401, Punjab, India; Department of Technical Sciences, Western Caspian University, Baku, Azerbaijan; School of Mechanical and Automotive Engineering, Qingdao University of Technology, 266520, Qingdao, China, e-mail: shubham543sharma@gmail.com, shubhamsharmacsirclri@gmail.com

2 — Kenya Kandwal *et al.* DE GRUYTER

BMO/rGO binary metal oxide/reduced graphene

composites oxide composites
BMOs Binary metal oxides

BTMOs Binary transition metal oxides

 $\begin{array}{lll} \text{CNT} & \text{Carbon nanotube} \\ \text{Co}_3\text{O}_4 & \text{Cobalt oxide} \\ \text{CoFe}_2\text{O}_4 & \text{Cobalt ferrite} \\ \text{Cu}_2\text{O}_3 & \text{Copper oxide} \\ \text{CuO} & \text{Copper oxide} \\ \text{CV} & \text{Cyclic voltammetry} \\ \text{DEG} & \text{Diethylene glycol} \\ \end{array}$

DI Deionized

DMF Dimethylformamide

EDLC Electrochemical double-layer

capacitor

ESS Energy storage system $F \cdot cm^{-2}$ Farad per square centimetre $FeSO_4 \cdot 7H_2O$ Iron(II) sulphate heptahydrate

 $\begin{array}{ll} \text{GO} & \text{Graphene oxide} \\ \text{H}_2\text{SO}_4 & \text{Sulphuric acid} \\ \text{HH} & \text{Hydrazine hydrate} \end{array}$

HNO₃ Nitric acid

HSC Hybrid supercapacitor KOH Potassium hydroxide

mA·cm⁻² Milliampere per square centimetre

 $\begin{array}{ll} \text{MEV} & \text{Mega electron volt} \\ \text{MnO}_2 & \text{Manganese dioxide} \end{array}$

MPa Megapascal

mS·cm⁻¹ Millisiemens per centimetre

NaNO₃ Sodium nitrate
NF Nickel foam
Ni₃S₂ Nickel sulphide
NiCo₂O₄ Nickel cobaltite
NiFe₂O₄ Nickel ferrite

NMP N-Methyl-2-pyrrolidone

PANI Polyaniline

PEDOT Poly(3,4-ethylenedioxythiophene)

Ppy Polypyrrole

PVP Polyvinylpyrrolidone
rGO Reduced graphene oxide
RUO₂ Ruthenium dioxide
SE Specific energy
SP Specific power

SEM Scanning electron microscopy

THF Tetrahydrofuran TiO_2 Titanium dioxide TMO Transition metal oxide V_2O_5 Vanadium pentoxide $W\cdot kg^{-1}$ Watt per kilogram

Wh⋅kg⁻¹ Watt-hour per kilogram

XRD X-ray diffraction
ZnO Zinc oxide

1 Introduction

With the widespread utilization of non-renewable fossil fuels and increasing concerns about global warming, the composition of the world's energy consumption is changing dramatically. The growth of environmentally friendly energy is currently prioritized over conventional fossil fuels [1,2]. Batteries, capacitors, and supercapacitors play a crucial role in the sustainable utilization of renewable energy sources by enabling the efficient storage of sustainable energy reserves for future uses. The most common kind of energy storage is a rechargeable battery, which stores energy by transferring charge between its electrodes via a redox process [3]. Batteries may be used as a steady power source for a short time, but they have a variety of drawbacks, including low power density, a limited life term, spark hazards, negative environmental effects, etc. [4]. The development of sustainable, clean, and green sources of energy has been prompted by ecological risks, high prices, and the diminishing supply of fossil fuels. Batteries and supercapacitors are the chosen superior choices to address the issue of using these renewable energy sources [5,6]. When it comes to energy storage systems (ESSs), power system operations are essential for reducing the intermittent nature of renewable energy supply and boosting system stability [7]. Thus far, interest has been shown in using supercapacitors and batteries, the two primary categories of electrochemical energy storage devices, for future energy storage applications. Because of their two outstanding qualities, long-term cycle stability, and high power output, supercapacitors are regarded as a fastgrowing new technology [8-10]. Nevertheless, compared to batteries, supercapacitors' potential future application is limited by their reduced energy content [11]. Supercapacitors, also known as power capacitors or ultracapacitors, are a type of green energy storage technology. This is due to the materials typically employed as the electrode and electrolyte in a supercapacitor [12]. Moreover, biowaste materials like coconut shells, eggshells, dead leaves, etc., can be used to create supercapacitors. In this regard, the supercapacitor also offers a productive and long-lasting alternative to recycle these bio-wastes, therefore reducing environmental contamination. It produces significantly

more specific energy (SE) than standard capacitors and relatively more specific power (SP) than batteries. It is intended to fill the gap between capacitors and batteries as a result. In addition, it has a longer lifespan and uses less energy than rechargeable batteries. Owing to these benefits, supercapacitors have received a lot of interest from researchers in a variety of industries and are anticipated to eventually replace batteries [13,14]. Current challenges in supercapacitor technology include low energy density and high cost. Future prospects involve increasing energy density, improving cycling stability, and integrating supercapacitors into renewable energy systems to reduce carbon emissions. The potential environmental impacts of supercapacitor materials include resource depletion, energy consumption during production, and waste generation.

Additionally, numerous strategies have been suggested to mitigate the possible adverse environmental effects of supercapacitor materials through sustainable synthesis methods, as an outcome of the synthesis techniques as well as material choices as stated following.

First, green synthesis methods, as the environmental impact of supercapacitor material production can be substantially reduced by employing green synthesis methods, such as hydrothermal, sol-gel, or microwave-assisted synthesis. These methods typically employ water as a solvent and moderate reaction conditions, thereby reducing waste generation as well as energy consumption.

Second, sustainable and biodegradable precursors, as the implementation of sustainable and biodegradable precursors into the synthesis process may further enhance sustainability. For instance, using biowaste-derived carbon sources or natural polymers as starting materials reduces dependence on fossil fuels and minimizes environmental impact.

Afterwards, recyclable materials, as the choice of recyclable materials for electrode synthesis can facilitate the recovery of materials and reuse, thus reducing waste formation and resource consumption. Materials such as metal oxides and reduced graphene oxide (rGO) are commonly recycled or repurposed in subsequent synthesis processes.

Fourth, energy efficiency, as it is imperative to optimize synthesis parameters in order to reduce energy consumption and achieve sustainability. In order to minimize energy consumption and preserve product quality, it is crucial to meticulously control process parameters, including temperature, pressure, and reaction time.

Fifth, life cycle assessment (LCA), as the identification of potential environmental hazards and the optimization of processes can be facilitated by conducting a comprehensive LCA of supercapacitor materials. LCA assesses the environmental impact of materials from the extraction of

primary materials to their disposal at the end of their lifecycle, thereby facilitating the development of rational choices and informed decision-making that mitigate the overall environmental impact.

Next, nontoxic solvents and additives, as the eco-profile of supercapacitor materials can be enhanced by substituting toxic solvents and additives with environmentally benign alternatives. Sustainable alternatives that mitigate environmental hazards throughout production and use include nontoxic binders and water-based electrolytes.

Finally, renewable energy sources, as the transition to renewable energy sources for synthesis methods, including solar or wind power, reduce greenhouse gas emissions and dependence on non-renewable resources, which aligns with sustainable development objectives.

In addition, sustainable synthesis methods can mitigate these impacts by using eco-friendly precursors, reducing energy consumption, and promoting recycling. Initially, the production process, as the environmental implications of the manufacturing of supercapacitor materials, particularly those that involve metals and metal oxides, is a concern. Energy-intensive apparatus and potentially hazardous compounds may be employed in processes such as solvothermal synthesis, hydrothermal synthesis, and chemical reduction. The procurement of basic materials, including metal precursors and graphene oxide (GO), may also raise concerns regarding resource depletion and mining practices. Next, during operation, as supercapacitors are frequently regarded as environmentally benign in comparison to batteries due to their absence of toxic heavy metals such as cadmium or lead. Nevertheless, the environmental impact of these devices during their operation is significantly influenced by the energy sources that are employed for powering them. The operation of these devices may result in indirect greenhouse gas emissions if the energy utilized for charging is derived from fossil fuels. Finally, disposal, in order to prevent environmental damage, supercapacitors may require appropriate disposal at the end of their lifecycle. Some materials, such as graphene, are relatively inert and have the potential for recycling. However, others, such as metal oxides, may present challenges in terms of appropriate disposal due to their potential to discharge hazardous substances into the environment if not handled properly.

H. I. Becker, born in 1957, used porous carbon electrodes to create a low-voltage capacitor [15,16]. The electric double-layer charge storage method was initially used in this energy storage device [17]. In 1966, Standard Oil of Ohio patents their supercapacitor concept. In 1971, NEC finally began to market the technology as a backup power source for computer memory under the moniker

"supercapacitor" [18,19]. After that, this field underwent a revolution, and several studies were conducted to enhance the functionality of the devices. Several businesses quickly entered the race to build supercapacitors, including Maxwell Technologies, NEC, Panasonic, ELNA, and others [20]. A high-capacitance hybrid supercapacitor (HSC) with carbon electrodes was created by FDK in 2007. The Kyoto Protocol and the Paris Climate Agreement set a 2060 deadline for reducing all emissions into the atmosphere resulting from the use of fossil fuels for energy. There will need to be a significant change in how energy is harnessed and used worldwide for this aim to become a reality. This goal can only be reached by integrating more energy sources that are renewable like wind, solar, and others. Thus, it is essential that fossil fuel-powered and nuclear power facilities be replaced [21-28]. Materials for carbon electrodes are a description of the most crucial electrode materials [29,30]. Together with certain novel materials that are available, the carbon materials are fully reviewed. In the contemporary nanoscale regime, nanotechnology has grown in significance and is used widely in industries including biology, computing, and sensors. This is a substance that has attracted a lot of interest recently due to its possible use in energy storage technology. rGO offers a few benefits over other materials when used as an electrode in a supercapacitor. Because rGO has a wide surface area, it has a big electrical charge storage capacity. Because supercapacitors are designed to swiftly store and release electrical energy, this makes them the perfect material for use in them. Because of its great electrical conductivity, the supercapacitor can be charged and discharged quickly. This material may be employed in a number of contexts because of its great stability and ability to endure several charging and discharging cycles without degrading. Overall, the performance and efficiency of these energy storage technologies might be greatly increased by using rGO as an electrode in supercapacitors [31,32].

In addition, the specific capacitance values obtained experimentally for various rGO-transition metal oxide (TMO) composites, such as rGO-MnO₂, rGO-Co₃O₄, and rGO-TiO₂, demonstrate that the incorporation of rGO with TMOs results in an increase in specific capacitance.

In terms of enhanced energy and power density, the composites exhibit superior energy and power density, which is crucial for high-performance supercapacitors due to their ability to facilitate efficient energy storage as well as rapid charge–discharge cycles. In terms of enhanced cyclic stability, several rGO–TMO composites demonstrate exceptional cyclic stability, with minimal capacitance degradation even after thousands of charge–discharge cycles, which underscores their long-term reliability and durability. In

terms of high rate capability, the composites are well-suited for applications that necessitate accelerated energy delivery, as they maintain a substantial capacitance at high current densities. In terms of novel electrode architectures, the utilization of rGO–TMO composites to fabricate flexible, 3D, or hierarchical electrode architectures provides adaptability and versatility for a variety of supercapacitor designs, such as wearable devices as well as flexible systems. In terms of synergistic effects, combining rGO with TMOs induces synergistic effects that strengthen the overall performance, electrochemical activity, and electron/ion transport in comparison to the individual components.

Moreover, the synergistic interactions between rGO and TMOs, as well as pseudocapacitive as well as double-layer capacitance effects, are the specific mechanisms that contribute to the enhanced electrochemical characteristics properties of rGO–TMO composites. Within the electrode materials, efficient charge transfer and ion diffusion are facilitated by factors such as the unique structural characteristics, high surface area, and conductivity of rGO. The rGO provides a conductive matrix and inhibits the agglomeration of TMO nanoparticles, thereby enhancing their electrochemical performance, while TMOs contribute to pseudocapacitance through redox reactions.

Furthermore, in the realm of energy storage technologies, supercapacitors have emerged as promising devices due to their high power density and rapid charge-discharge capabilities, making them ideal for various applications. This article delves into the realm of electrochemical supercapacitors, focusing on the synthesis and electrochemical performance of binary transition metal oxide (BTMO) and rGO composite materials. By exploring the production processes and synergistic advantages of binary metal oxide (BMO)-rGO composites, this study sheds light on how these composites surpass individual components in terms of specific capacitance and cycle stability. The research underscores the potential of BMO-rGO composites as superior electrode materials for supercapacitors, showcasing their enhanced specific capacitance, improved charge storage capacity, increased power density, exceptional cycling stability, and sustained durability even after extensive chargedischarge cycles.

Composite materials with enhanced electrochemical characteristics that are appropriate for supercapacitor applications are the primary novelty, which is the synergistic combination of rGO with a variety of TMOs. Compared to individual TMOs or other carbonaceous materials, these composites demonstrate enhanced specific capacitance, energy density, power density, cyclic stability, and rate capability. The synthesis processes and synergistic benefits of BMO-rGO composites are discussed, with an

emphasis on their superior performance in specific capacitance and cycle stability compared to individual components. This research highlights the potential of BMO-rGO composites as high-performance electrode materials for supercapacitors, showcasing their enhanced specific capacitance, improved charge storage capacity, increased power density, excellent cycling stability, and overall durability even after numerous charge-discharge cycles.

1.1 Supercapacitors

A supercapacitor comprises two electrodes separated by an ion-permeable layer termed a separator, yet electrically coupled by an electrolyte. A substance called the electrolyte contains both positive and negative ions [33,34]. To link the two electrodes with the electronic circuit, a thin metallic layer known as a collector is put on their outer surfaces and a separator allows ions to move between the electrodes while maintaining their electrical isolation. Supercapacitors may be divided into three groups based on their high-energy storage mechanisms: electrostatic double-layer capacitors (EDLCs), hybrid capacitors, and pseudocapacitors [35]. In EDLCs, ions from the electrolyte adsorb to the surface owing to electrostatic attraction, storing the charges and generating two charged layers (double layer). The essential criteria for EDLC electrodes are large surface area, good conductivity, and quick charge/discharge rates. These materials come in a variety of shapes and sizes, including powders, tubes, composites, aerogels, and sheets. They are nontoxic, have a large surface area, and have adjustable porosity and strong electrical conductivity. Carbon-based electrode materials are typically used to create EDLCs. Through quick and reversible oxidation and reduction processes, pseudocapacitors store charges. The extra charges that are transmitted within the prescribed potential, pseudocapacitors exhibit larger capacitance than EDLC-type gadgets, but they often have lower cycle lives owing to active material deterioration brought on by Faradaic reactions. Due to their quick reversible low cost, redox reaction, metal oxides, and simple processing, conductive polymers can be utilized as pseudocapacitive electrode materials [36]. However, despite these benefits, pseudocapacitive electrode materials' inherent low energy density has been a barrier to their ability to surpass batteries for broad commercial applications [37–39]. However, because of their lesser energy density when compared to batteries, ultracapacitors are mostly employed as backup power sources to support batteries in electric cars [40]. Other than electric vehicles, supercapacitors are employed in drills that supercapacitors are used by

astronauts to repair the International Space Station while they are on spacewalks [41–43]. Additionally, the emergence of next-generation flexible, wearable electronics, and portable optoelectronics devices necessitates miniaturized ESS with distinct advantages of light weight and flexibility [44-49]. As a result, there is a massive push to the increment of the energy density of supercapacitor technologies, currently 5-35% when compared with Li-ion batteries, that can be further used for industrial purposes. Asymmetrical supercapacitors (ASCs) are supercapacitors that, in contrast to conventional supercapacitors, have two electrodes that are different from one another: a cathode that functions as a battery-type Faradaic energy source and an anode that functions as a capacitor power source. When aqueous electrolytes are utilized, the operational voltage of a symmetric supercapacitor is often restricted to less than 1.0 V due to the thermodynamic breakdown potential of water molecules. Nevertheless, by utilizing organic electrolytes, the operating voltage may be increased above 2.5 V. For certain uses, however, these organic electrolytes might be poisonous and not environmentally friendly. Hence, using two distinct electrode materials for the anode and the cathode is a practical way to increase the operating voltage for aqueous electrolytes. Because of the greater operating voltage, ASCs were able to reach a higher energy density. The energy density termed as E [50-54] is given by

$$E = 1/2CV^2$$

The specific capacitance termed as C of a super-capacitor can be increased by enhancing the inherent properties, such as electrical conductivity, chemical stability, and porosity of the electrode materials, as well as low-dimensional nanostructures (sheets, nanorods, foams, quantum dots, etc.), and electrode designs.

1.2 Graphene and its derivatives

Due to its distinct structure and features, graphene of sp² hybridized carbon atoms has shown considerable potential in a number of applications [55,56]. It is semi-metallic in composition and has a bond length of 1.42 C-C. Many scientific and technical investigations have been prompted by the special features of graphene [57]. Due to the semimetal composition of graphene, charge carriers act like Dirac fermions [58], producing astonishing phenomena including increased mobility up to 2,000 cm²·s⁻¹ [59]. The distinctive qualities of graphene, viz. graphene or GO is covered with epoxy functional groups and also with hydroxyl, and it has a higher mechanical stiffness of 1,060 GPa, a thermal conductivity of 5,000 W·m⁻¹·K [60], a large surface area of $2,630 \text{ m}^2 \cdot \text{g}^{-1}$, an intrinsic mobility of 200,000 cm²·V⁻¹·s⁻¹ [61], and an excellent optical transmittance of 97.7% [62]. This has led to a large number of investigations for numerous technological applications. Sp3 bonding is severely disrupted during the oxidation process, significantly reducing the electrical conductivity of GO in comparison to graphene [63-65]. Hummers and Offeman [66], Brodie (1859) [67], or Staudenmaier [68] described strategies for producing GO. Toxic and explosive-reducing agents, such as hydrazine hydrate (HH) [67] and sodium borohydride [68], are frequently utilized in the reduction of GO to rGO. Any organic solvent may be used to exfoliate graphite oxide to create GO, resulting in GO in a variety of forms with varying levels of long-term stability and single-layer thickness. A single layer of GO sheet may be formed using a single layer of four different types of organic solvents, including dimethylformamide (DMF), NMP, THF, and ethylene glycol [69]. The oxidation of GO in the molecule and the production process are also factors that affect its conduction capacity. GO sheets are mechanically robust membranes with millions of tiny flakes that can be distributed in water and other organic solvents like DMF and oxygen-containing epoxide groups [70]. The most intriguing characteristic of GO is that it can be reduced to rGO sheets by removing the oxygen-containing groups with a re-developing p-conjugated structure. Graphene has several features including high thermal conductivity, high surface area, remarkable transparency, ultrahigh electric conductivity, and good mechanical strength. Bulk graphite can be converted into single-layer and few transferable graphenes by thermal reduction of GO [71-73], mechanical or ultrasonic exfoliation [74], epitaxial chemical vapor deposition [75], epitaxial growth [76], plasma enhancement [77], electric arc discharge [78], epitaxial growth, and chemical intercalation. The synthesis of graphene in large numbers and at a reasonable price via the chemical reduction of GO is acknowledged [79]. Graphene has gained popularity and is a substance with many possible uses. It is used in sensors [80], supercapacitors [81], hydrogen storage [82], coatings [83], composites [84], paint ink [85], dye-sensitized solar cells [86,87], transparent conductive layers [88], bio-applications [89,90], and drug delivery [91]. This is because of its special transport properties and physicochemical properties. A graphene derivative known as rGO is created by reducing GO. Graphene's key properties that make it suitable for energy storage in supercapacitors include its high electrical conductivity, large surface area, excellent mechanical strength, and chemical stability. However, the potential for enhancing the performance and efficacy of energy storage technologies is presented by the incorporation of graphene and its derivatives in supercapacitors. When combined with a variety of metal oxides and other materials,

graphene is an optimal platform for enhancing the electrochemical properties of supercapacitors due to its exceptional electrical conductivity, large surface area, and mechanical strength. The following remarks have been inferred from the literary studies:

a. rGO-MnO₂ composite:

In order to enhance mechanical stability and electrical conductivity, rGO is combined with MnO_2 , a pseudocapacitive material that possesses an exceptional specific capacitance.

This composite is highly suited for high-performance supercapacitors due to the synergy among MnO₂ and rGO, which achieves a balance between power density and energy density.

b. rGO-Co₃O₄ composite:

In order to enhance capacitance efficacy, rGO is combined with Co_3O_4 , an additional pseudocapacitive material.

The rGO-Co₃O₄ composite is a promising candidate for next-generation supercapacitors due to its enhanced cyclic stability as well as particular capacitance.

c. rGO-TiO₂ composite:

TiO₂, which is renowned for its stability as well as extensive surface area, is combined with rGO in order to enhance the stability of cycles as well as the capacity of charge storage.

The potential of the rGO–TiO₂ composite for supercapacitor applications is suggested by its superior electrochemical performance in comparison to pure TiO₂.

d. rGO-ZnO composite:

In order to enhance the rate capability and cycle performance, rGO is integrated with ZnO, a wide-bandgap semiconductor.

Both electric double-layer capacitance (EDLC) and pseudocapacitive contributions are demonstrated by the rGO–ZnO composite, which maintains a high level of capacitance even after numerous charge/discharge cycles.

e. $rGO-Ni_3S_2$ composite:

Ni₃S₂, a material that has the potential to be used in pseudocapacitors, is combined with rGO to enhance its energy storage capabilities.

The $rGO-Ni_3S_2$ composite is well-suited for highrate applications due to its exceptional cyclic stability as well as particular capacitance.

f. rGO-NiCo₂O₄ composite:

rGO has been combined with $NiCo_2O_4$, a mixed metal oxide that exhibits a high pseudocapacitance, to obtain optimal performance.

The rGO-NiCo₂O₄ composite has the potential to be employed in a variety of supercapacitor applications

due to its superior cyclic stability as well as elevated specific capacitance.

g. rGO-ZnCo₂O₄ composite:

ZnCo₂O₄ exhibits outstanding characteristics in terms of cyclic stability and energy density when combined with rGO

Promising energy storage capabilities are presented by the rGO-ZnCo₂O₄ composite, a practicable material option.

h. rGO-RuO₂ composite:

RuO₂, which is recognized for its high specific capacitance, is incorporated into rGO to enhance the performance of energy storage.

rGO-RuO₂ composites are well-suited for applications that necessitate high energy density due to their superior cyclic stability as well as elevated specific capacitance.

Thus, the electrochemical performance of supercapacitors is enhanced by the incorporation of graphene as well as its derivatives in conjunction with a variety of metal oxides and materials. This results in enhancements in specific capacitance, cyclic stability, rate capability, and energy density. In order to optimize these composite materials for specific application requirements and performance criteria, additional studies and experiments are required.

Moreover, utilizing graphene and its derivatives in supercapacitors can enhance performance and efficiency by increasing specific capacitance, improving charge/discharge rates, enhancing cycling stability, and reducing overall system weight and size. Graphene's exceptional surface area allows for the efficient adsorption of ions and provides a large number of sites for charge accumulation. Supercapacitors' specific capacitance is significantly improved by this property. Graphene's high electrical conductivity facilitates the rapid transport of electrons within the electrode material. Low internal resistance is an outcome of this characteristic, which enables high-rate chargedischarge processes, which are essential for attaining high power densities. The exceptional mechanical strength and flexibility of graphene render it an ideal material for the development of supercapacitor electrodes that are both flexible and robust. Even in the presence of mechanical stress or deformation, this property assures the device's durability and longevity. The chemical stability of graphene is characterized by its resistance to corrosion and its inertness in a variety of electrolytes. The device's reliability and lifespan are enhanced by this stability, which prevents electrode degradation and promises long-term performance. Graphene can be readily functionalized or combined with other materials to enhance certain characteristics,

including ion storage capacity or pseudocapacitance. The design of electrode architectures that are specifically tailored to satisfy specific performance requirements is facilitated by this compatibility. Graphene frequently demonstrates synergistic effects that enhance the electrochemical performance of supercapacitors when it is combined with TMOs or other nanomaterials. Furthermore, these synergies may result in enhanced cycling stability, specific capacitance, and rate capability.

1.3 BMOs

BMOs have important uses in energy storage, notably in supercapacitors. Two distinct transition metal elements are joined with oxygen to form BMOs. In comparison to other materials, they have a superior high reversible capacity, enhanced electronic conductivity, and structural stability. BMOs have received substantial research as innovative super-capacitor electrode materials. Pseudocapacitors, which include BMOs, offer more specific capacitance and energy density than double-layer capacitors. The increasing demand for energy storage options has led researchers to further investigate BMO materials. Compared to other materials, they have a higher capability for reversibility. Supercapacitors' total capacity for energy storage is increased by this characteristic, which enables them to store and release more charge throughout the charge-discharge cycle. Their improved structural stability ensures their lifetime even after several charging and discharging cycles. The life cycle of super-capacitor electrodes and the maintenance of constant performance depends on this stability. Fast charge/discharge rates and greater energy storage capability are both affected by increased conductivity [92–94].

1.4 rGO and BMO composite

For nanosized active material particles, graphene and its derivatives, such as GO and rGO, have been recognized as potential carbonaceous supporting materials [95-97]. Composite materials might be predicted to perform better in batteries because 3D porous rGO frameworks can efficiently maintain the integrity of composite materials and enhance charge/electrolyte transfer during electrochemical reactions. Additionally, 2D GO sheets are simple to process as a precursor for rGO, and their rich surface functional groups make them to electrostatically trap metal ions, which are often used as the metal source for BMO crystals.

Therefore, following further treatments, BMOs will begin to form on the side of the surface of rGO. BMO development and 3D rGO frameworks are often done separately. As a result, the rGO sheets will not be able to enclose the TMO crystal. BMO/rGO composites with various structural characteristics have been created by combining the metals' GO reducing agent with Zn, Sn, and Fe as TMO precursors. rGO plays a crucial role in supercapacitors by providing a conductive network, increasing surface area for charge storage, improving electron transfer kinetics, and enhancing the overall electrochemical stability of the electrodes. rGO/BMO composites enhance supercapacitor performance by preventing graphene restacking, increasing specific capacitance, improving charge storage capacity, and enhancing overall electrochemical performance. As far as the synergistic effect is concerned, the electrochemical performance is substantially enhanced by the integration of BTMOs with rGO, resulting in a synergistic effect that cannot be achieved by either component independently. The pseudocapacitive or double-layer capacitance behaviour of the BTMOs, in conjunction with the high surface area and electrical conductivity of rGO, results in this synergy. As far as the increased conductivity is concerned, the electrode structure is facilitated by the remarkable electrical conductivity of graphene-based materials such as rGO, which allows for rapid electron transport. The supercapacitor's overall performance is enhanced by the efficient charge/discharge processes that are enabled by the high conductivity, which reduces internal resistance. As far as the surface area is concerned, the supercapacitor's capacitance is significantly enhanced by the extensive surface area available for ion adsorption and desorption, which is facilitated by the layered structure of graphene. Additionally, the electrochemical activity of graphene is further enhanced by the presence of functional groups and defects on its surface, which facilitates redox reactions and promotes ion accessibility. In terms of pseudocapacitive behaviour, numerous BTMOs demonstrate pseudocapacitive behaviour, which entails the ability to store charge through faradaic redox reactions at the electrode-electrolyte interface. The pseudocapacitive properties of BTMOs are effectively realized when combined with rGO, which facilitates ion diffusion and provides a conductive framework. This results in a higher energy density and capacitance. As far as the enhanced cyclic stability is concerned, the robust electrochemical performance and stable structure of rGO/ BTMO composites contribute to enhanced cycling stability. The BTMO nanoparticles are prevented from agglomerating and undergoing structural degradation during charge/ discharge cycles by the graphene matrix, which functions as a mechanical support. Consequently, the long-term

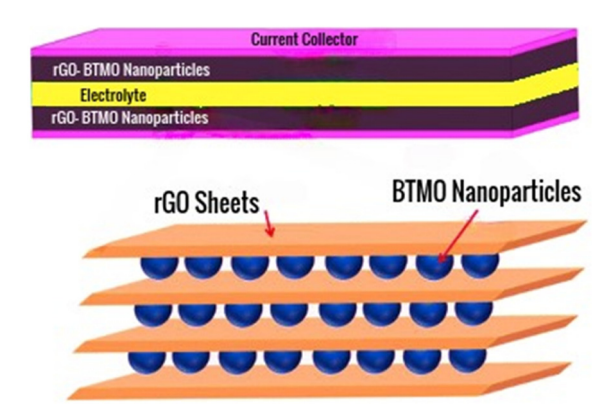


Figure 1: rGO/BMO composite.

performance of the system is preserved. As far as the tailored nanocomposite design is concerned, the synthesis method and the specific choice of BTMO can be customized to optimize the performance of rGO/BTMO composites for specific applications. The electrochemical characteristics of the nanocomposite can be optimized to match the desired specifications by modifying parameters such as the composition ratio, particle size, morphology, and surface functionalization. As far as the scalability and cost-effectiveness is concerned, the production of graphene-based materials is becoming more cost-effective and scalable, particularly as a consequence of developments in synthesis techniques. The versatility of BTMOs, in conjunction with the scalability of rGO/BTMO composites, renders them promising candidates for large-scale energy storage applications, such as supercapacitors, where cost and performance are critical factors. These BMO/rGO composite preparation techniques are simpler, more efficient, and environmentally beneficial. As a consequence, these BMO/ rGO composite electrodes have produced excellent storage characteristics (Figure 1).

2 Synthesis method

2.1 Synthesis method for GO and rGO

Brodie's method: GO was originally created by Brodie in 1859; therefore, the process has a lengthy history. By mixing potassium chlorate (KClO₃) with a mixture of graphite flakes in fuming nitric acid (HNO₃), Brodie suggested creating GO. In a glass beaker, graphite flakes were combined with nitric acid and fuming potassium chlorate, and the lass beaker thereafter was submerged in an ice bath to maintain temperature. After continuous stirring, graphite

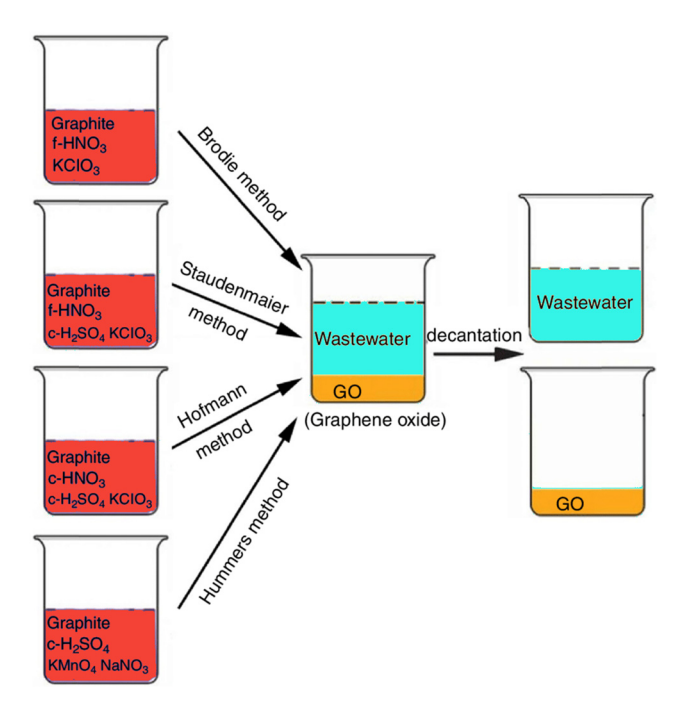


Figure 2: Different synthesis methods of GO.

flakes became fully oxidized. Afterwards, to remove contamination and acid, it was rinsed with DI water and centrifuged. The final product which is dark brown powder was vacuum-dried to remove moisture. It produces GO with less impurity and forms GO with a higher degree of oxidation. The major drawbacks of this experiment where it was more aggressive and harmful (Figure 2) [98].

GO preparation with the Staudenmaier method: Staudenmaier improved Brodie's procedure in 1898 by adding concentrated sulphuric acid (H2SO4) to boost reaction acidity instead of a single addition of KClO3 and many applications of KClO₃ during the reaction. GO was produced using the Staudenmaier technique. By distilling a solution of concentrated HNO3 and concentrated H2SO4 (1:3), fuming nitric acid was created. Vacuum distillation is used to repeatedly purify the nitric acid. Using a pycnometer, the concentration of fuming nitric acid was measured. A reaction flask with a magnetic stir bar, a mixture of 87.5 mL of H₂SO₄ (98% concentration) and 27 mL of fuming HNO₃ was formed. The mixture was placed in an ice bath for 30 min to settle. To prevent agglomeration and create a homogenous dispersion, 5 g graphite was gradually added and vigorously stirred before adding 55 g of KClO₃. After completion, the flask was then loosely covered to allow the gas to escape from the solution. At room temperature, the sample was forcefully agitated for 96 h. Once the reaction was finished, the mixture was decanted into 3 L of deionized water. The sulphate ions were subsequently

removed by redispersion in HCl (5%) solutions, centrifugation, and redispersion in deionized water many times till a negative reaction on sulphate ions and chloride was accomplished and was dried for 48 h at 60°C in an oven [99].

Making graphite oxide using the Hofmann technique: $\mathrm{HNO_3}$ (27 mL, 68%) and $\mathrm{H_2SO_4}$ (87.5 mL, 98%) were added into a flask and chilled in an ice bath for 30 min. To prevent explosive chlorine dioxide gas production and sudden temperature rise, add 5 and 55 g graphite to an ice bath in the reaction flask. The mixture was stirred continuously for 96 h, and then the mixture was decanted into 3 L of deionized water. GO is then redistributed in HCl solutions to remove the sulphate ions. Graphite oxide slurry was dried in an oven at 60°C for 48 h before use [100,101].

Hummer's technique of preparing graphite oxide: $2.5\,\mathrm{g}$ of NaNO $_3$ and $115\,\mathrm{mL}$ of DI water were mixed with $135\,\mathrm{g}$ of graphite with 98% H $_2\mathrm{SO}_4$. A subsequent ice bath was used to settle the mixture. Afterward, $15\,\mathrm{g}$ of KMnO $_4$ was well stirred. During the course of $2\,\mathrm{h}$, the reaction mixture was allowed to warm up to room temperature prior to being heated for $30\,\mathrm{min}$ at $35\,^\circ\mathrm{C}$ for $4\,\mathrm{h}$. The reactions were added to a flask containing $250\,\mathrm{mL}$ of deionized water and then heated for an additional $70\,^\circ\mathrm{C}$. Then, the mixture was held constant for around $20\,\mathrm{min}$ before being transferred to $1\,\mathrm{L}$ of DI water. The reaction mixture was decanted after settling. Then, it was redistributed in DI water after being repeatedly centrifuged and cleaned. Afterward, the graphite oxide solution was dried for $48\,\mathrm{h}$ at $60\,^\circ\mathrm{C}$ in the oven before use [102-105].

Modified Hummer's method: A 500 mL flask was filled with 2 g of pure graphite flakes, 1 g of NaNO₃, and 45 mL of sulphuric acid. The flask was placed in an ice bath with constant stirring for 30 min and monitored to prevent temperature from exceeding 15°C. After homogenizing the mixture, 6 g of KMnO₄ was added. After the ice bath is removed, the temperature of the mixture steadily rises. The mixture was kept like this for 30 min until it began to thicken and turn into a dark green paste. Afterward, 80 mL of DI water was gradually added while stirring. Both a rapid rise in temperature and violet effervescence were seen at the same time. The mixture was stirred on a hot plate for 30 min at 90°C. The solution was diluted by adding 200 mL of DIW. The colour of the solution changed to bright yellow with the addition of $3 \,\mathrm{mL}$ of $\mathrm{H}_2\mathrm{O}_2$. The mixture was centrifuged and repeatedly rinsed with 100 cc of 10% HCl to remove the metal ions. To remove the supernatant, the solution was centrifuged for 20 min at 4,000 rpm. Once the pH reached neutral, this process was done multiple times. By utilizing ultrasonication, the resulting graphite solution was exfoliated to GO. Finally,

the GO solution was maintained at 50°C in a petri dish for 24 h [106,107].

Creation of GO by Tour Approach: At a ratio of 9:1 (v/v), concentrated H₂SO₄ (sulphuric acid) and concentrated H₃PO₄ (ortho-phosphoric acid) were combined to create GO. Phosphoric acid is added to prevent further oxidation. Adding 0.50 g graphite powder and 4.5 g KMnO₄ (potassium permanganate) to the acid mixture, results in temperature changes ranging from 40°C to 50°C. A temperature-controlled water bath was used to get the mixture to 50°C, followed by 12 h of stirring. The mixture transformed into paste as the process continued. After 12 h, the liquid was cooled to room temperature, and to terminate the process, 250 mL of distilled water was added. The manganese ion was reduced to soluble manganese sulphate (MnSO₄) and manganese oxides by adding 10 mL of 30 wt% H₂O₂. The following procedure used H₂O₂ to convert residual KMnO₄ to soluble MnSO₄ in an acidic media. When 30 wt% H₂O₂ was injected, bubbling and a bright yellow hue seen appeared, indicating a significant amount of oxidation. A graphite oxide (GTO) filter cake was formed after the solution was filtered to remove the metal sulphate using filter paper. The cake was thoroughly cleaned with a 5% HCl aqueous solution to remove all the sulphate ions. Using BaCl₂ solution, the removal of metal sulphate ions was verified. The supernatant was decanted and used to wash again after 4 h of centrifugation at 4,000 rpm. The pH of the obtained sample was tested using a universal indicator. The collected material (GTO) was agitated in distilled water for 12 h at 60°C. This process is referred to as exfoliation [108].

Table 1 summarizes various synthesis methods for producing GO. Each procedure specified here has specific requirements and reagent compositions. Graphite, NaNO₃, KMnO₄, H_2SO_4 , H_3PO_4 , H_2O_2 , HNO_3 , and KCl are used to prepare GO, which is then reduced to rGO. These approaches provide many ways to synthesize GO and rGO, each with advantages and disadvantages that are tailored to certain research requirements and applications in the field of graphene-based materials.

2.1.1 Synthesis of rGO-TiO2 composite

The process of synthesizing $rGO-TiO_2$ nanocomposites involves combining titanium dioxide (TiO_2) nanoparticles and nanobelts with chemically rGO. The synergistic effects of both components are harnessed by fabricating these nanocomposites with a meticulously controlled mass ratio of TiO_2 to rGO, which is typically optimized at 3:7.

In order to ensure that the rGO sheets and TiO_2 nanoparticles are in close proximity, nanocomposite synthesis is typically conducted using chemical methods, including hydrothermal or sol–gel techniques. The mesoporous TiO_2 offers a high surface area and active sites, which contribute to higher specific capacitance and cycle stability, while the rGO functions as an ion reservoir, allowing electron mobility during charge transfer.

2.1.2 Electrochemical characteristics of the rGO-TiO₂ composite

The electrochemical efficacy of rGO–TiO₂ nanocomposites is excellent and is crucial for supercapacitor applications. In particular, these composites demonstrate:

- i. Rate capability enhancement: The composite's rate capability has been enhanced by the combination of rGO with TiO₂ nanobelts, which enables rapid charge/discharge processes at high current densities. This is because TiO₂ nanobelts have a high concentration of active sites, and rGO provides efficient electron transport channels.
- ii. High specific capacitance: The rGO–TiO₂ nanocomposites have higher specific capacitance values, particularly at moderate current densities, than pure TiO₂. This is due to the synergistic effects of rGO and TiO₂, in which rGO functions as a conductive scaffold, thereby enabling the storage of charge within the composite structure.
- iii. Enhanced energy density and power density: The tailored morphology and composition of rGO–TiO₂

Table 1: Different methods for GO with precursor required

Method	Graphite (g)	NaNO ₃ (mL)	KMnO ₄ (g)	H ₂ SO ₄ (mL)	H ₃ PO ₄ (mL)	H ₂ O ₂ (mL)	HNO ₃ (mL)	KCI (g)	References
Staudenmaier method	5	_	55	87.5	_	_	27	_	[109]
Hoffmann	5	_	_	87.5	_	_	27	55	[110]
Hummer's method	13.5	2.5	15	_	_	_	_	_	[111–114]
Modified Hummer's method	2	1	6	45	_	3	_	_	[115–118]
Tour method	0.5	_	4.5	90	10	10	_	_	[119]

composites aid in an enhancement of energy density and power density, which are essential metrics for assessing supercapacitor performance. The composite's hierarchical structure enables high-energy storage capacities by ensuring effective ion diffusion and electron transport.

iv. Long-term stability: The rGO-TiO₂ nanocomposites demonstrate exceptional cycling stability, maintaining a substantial portion of their initial capacitance during extended charge/discharge cycles. This is due to the robust interfacial interactions between rGO and TiO₂, which reduce electrode degradation while maintaining electrochemical performance.

Thus, integrating rGO with TiO_2 nanoparticles and nanobelts presents a promising opportunity to advance supercapacitor technology by leveraging the distinctive characteristics of each component to accomplish superior electrochemical performance. Optimizing synthesis parameters and composite form can improve $rGO-TiO_2$ composites' efficacy and application in energy storage devices.

2.2 Synthesis method for BMO composite

Hydrothermal/solvothermal synthesis: It is the production of BMOs using solvents under high pressure and temperature to dissolve and recrystallize minerals. To obtain vapour saturation pressure, temperatures are often greater than 100°C, and the products are additionally affected by liquids and dissolved salts. This process can synthesize a wide variety of multi-part oxide materials and BMO with typical low-temperature phases and oxidation states, making it an attractive option for low-cost BMO manufacture. It has benefits including an inexpensive precursor, low-temperature processing, and a simple process. Additionally, the solvothermal approach produces highly mono-dispersed particles having adjustable shape and size while avoiding the need for dangerous catalysts. It provides a variety of BMOs with porous surfaces and huge specified regions (Figure 3) [120].

Microwave-assisted method: A quick approach for producing bimetallic oxide nanoparticles (BMOs) with adjustable structure, size, and morphology is the microwave-assisted method. The one-pot production of several bimetallic oxide nanoparticles and nanostructures, including MFe_2O_4 (M=Zn, Ni, Mn), and $NiCo_2O_4$, has often utilized this technique. It has benefits including regulated heating, a faster response rate, quicker reaction times, and improved product yields. Controlling the shape and phase of BMOs, however, may be challenging. The coupled microwave-solvothermal approach combines the benefits of microwave and solvothermal conditions, resulting in a significant decrease in reaction time, control over morphology, and the production of very pure, narrow-size-distribution

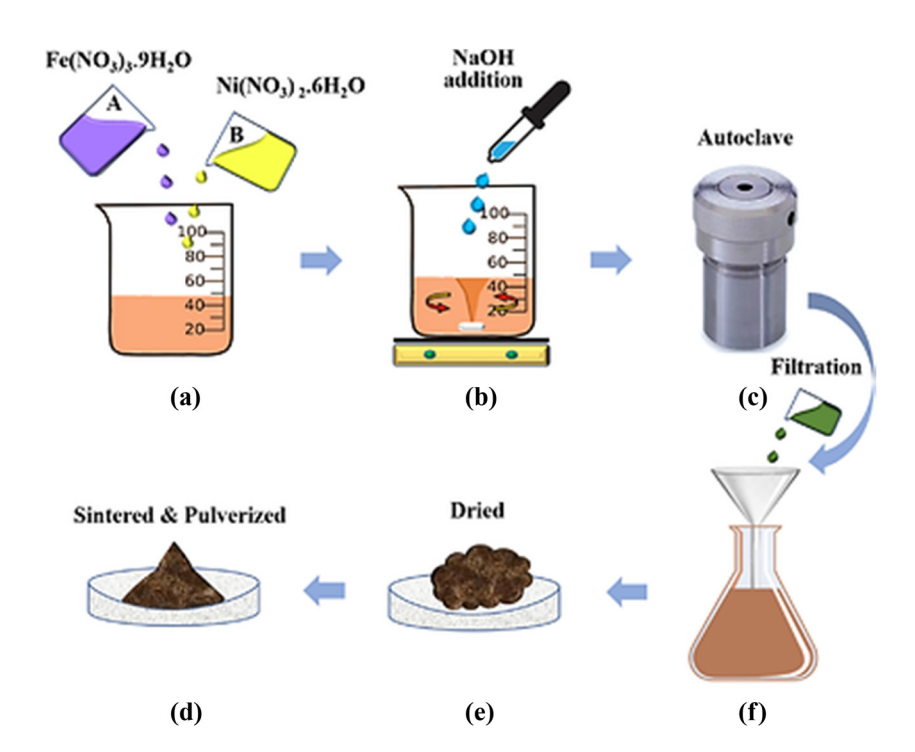


Figure 3: Hydrothermal process for NiFe₂O₄. Reproduced with permission from the study of Anik et al. [121].

particles. For crystallizing BMOs with regulated phase and shape, this method works well (Figure 4).

Electrodeposition method: This requires only one synthesis step throughout the entire process. The basis for electrodeposition is electrochemical redox reactions, in which an electric current flows through a metal salt solution, depositing the metal at the cathode. Even at room temperature, this method can increase gravimetric and volumetric energy density while eliminating ohmic resistance. The most well-known use of the process is the electro-reduction of cobalt and nickel nitrate mixtures to produce NiCo₂O₄. There have been reports of several conductive substrates, including carbon fibre, stainless steel, nickel foam (NF), and carbon fabric. NiCo2O4 arrays on flexible carbon fibre have proved remarkable electrochemical storage capabilities after 3,000 cycles of high stability. Finally, electrodeposition offers a straightforward technique for producing BMOs with a consistent shape, but with limitations in small-scale manufacture [122].

Template method: Mesostructured BMOs are helpful for electrochemical materials because of their variable pore diameters, morphologies, and large surface areas. Because of these characteristics, liquid electrolytes diffuse into electrode materials by increasing contact between the electrolytes and the electrode. Thermal instability rendered BMOs ineffective. For the synthesis of mesostructured BMOs, the template approach is often combined with the solvothermal/hydrothermal method. Hard-template and soft-template techniques are two categories of template-directed procedures. Due to their tetra-connected covalent bonds, rigid templates like silica are often utilized because they provide highly organized nanoscale structure and homogeneous pore size distributions. Yuan et al. created

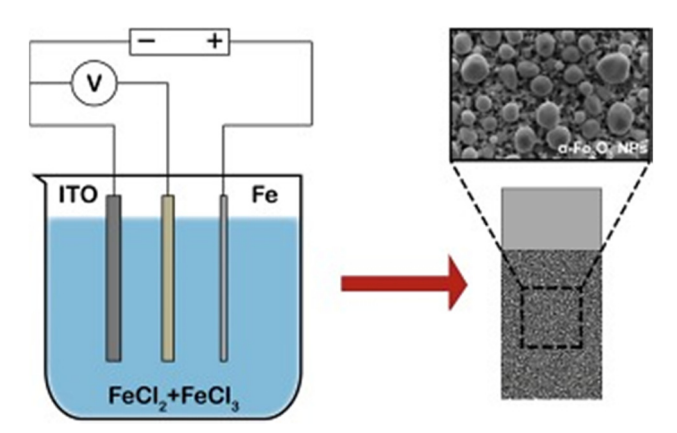


Figure 5: Electrodeposition method for Fe_2O_3 . Reproduced with permission from the study of Meng et al. [123].

using silica spheres ultra-thin mesoporous hollow NiCo_2O_4 structures. These structures feature a high specific capacitance and excellent long-term cycle stability at high current densities. Flexible organic molecules, surfactants, block copolymers, and microemulsions are examples of soft-template techniques that act as structure-directing agents throughout the synthetic process. They offer several benefits, including being affordable and simple to build without sophisticated facilities. Jan's group developed a thin-film electrode of nickel molybdate with a 3D honeycomb structure to improve lithium-ion storage capacities. Studies have shown that the synthesized PVP as a capping agent for mesoporous NiCo_2O_4 , controlling an-isotropic development and bringing particles together to produce specialized NiCo_2O_4 (Figure 5) [124,125].

Sol-gel method: Due to the adjustable purity, composition, homogeneity, and temperature of the sol-gel approach, binary complex metal oxides (BMOs) are often synthesized

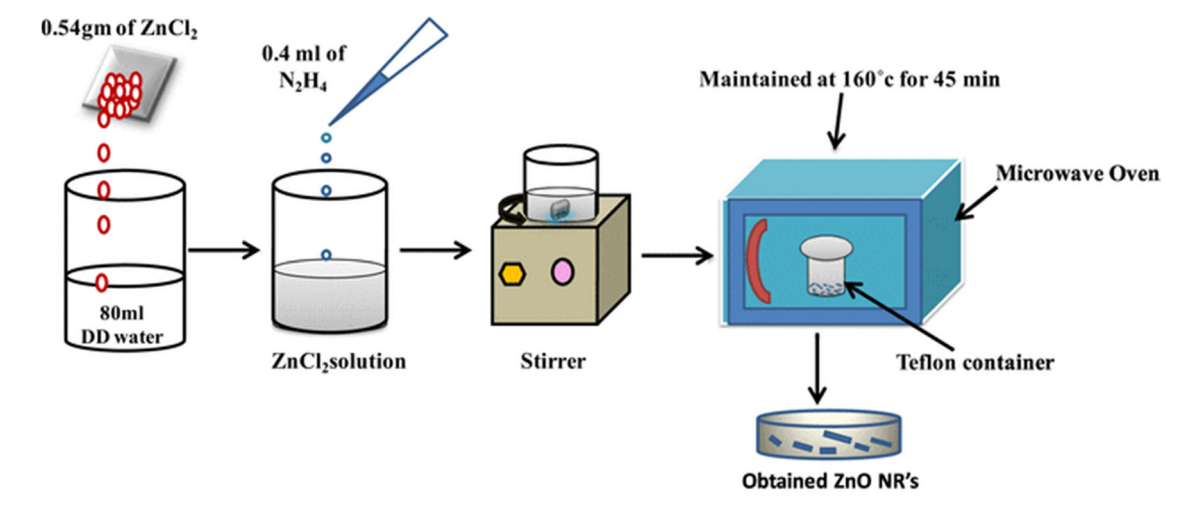


Figure 4: Microwave synthesis method for ZnO. Reproduced with permission from the study of Senthilkumar et al. [126].

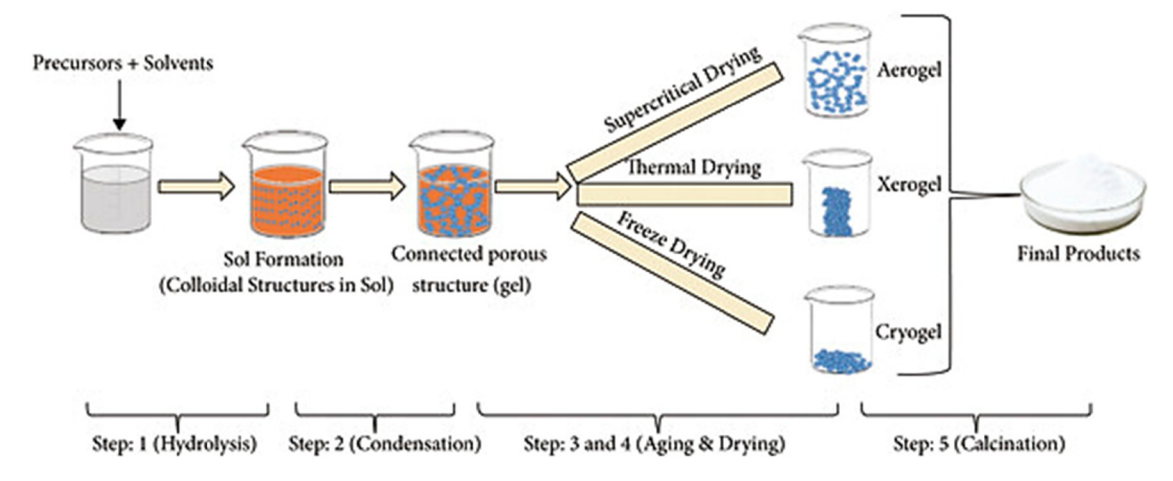


Figure 6: Sol-gel synthesis method. Reproduced with permission from the study of Bokov et al. [127].

using this technology. However, the necessity for significant quantities of organic solvents and reagents makes large-scale applications difficult. Hu et al. previously developed $\rm NiCo_2O_4$ aerogels with the potential to be used as supercapacitor electrodes and a homogeneous shape. An $\rm NiCo_2O_4$ framework resembling a 3D hierarchical porous network was created by Yuan et al. to provide an electron transport channel. This method offers a potential synthetic approach. This method offers a practical approach to the synthesis of additional BMOs (Figure 6) [128].

2.3 Synthesis method for rGO BMO composite

Hydrothermal: A method of preparing $rGO-NiFe_2O_4/NF$ electrodes. After being washed and dried, commercial NF was impregnated with a mixture of $FeSO_4\cdot7H_2O$, $Ni(NO_3)\cdot26H_2O$, and $CO(NH_2)_2$, followed by the addition of rGO colloidal solution. The mixture was heated at $180^{\circ}C$ for 12 h in a Teflon-lined stainless-steel autoclave, then cooled and cleaned using deionized water and ethanol. To create the $rGO-NiFe_2O_4/NF$ composites, the resulting $NiFe_2O_4/rGO$ layered double hydroxide is heated at $350^{\circ}C$ for 2 h (Figure 7) [129,130].

Sol-auto combustion process: In this method, nickel nitrate hydro-oxide, ferric nitrate, and glycine NH₂CH₂ COOH were the materials used to prepare the precursor solution, 50 mL of deionized water was first dissolved in the stoichiometric quantity of nickel and iron nitrates at a 1:2 Ni/Fe molar ratio. A 50 mL aqueous solution of glycine was prepared, and a 1:1 molar ratio of cation to fuel agent was introduced while stirring continuously to a solution of metal precursors. The final solution, which had a pH of 3.0–3.5, was agitated at 300 rpm for 1 h at 70–80°C to

remove any remaining water. An aqueous ammonia solution was added drop by drop until the precursor solution's pH reached 7. Once a viscous solution had formed, it was dried to produce a gel. The gel was placed on a hot plate preheated to 300°C and cooked until it lit. When a colloidal solution of GO was introduced to the metal salt combination before the fuel agents, complex oxide/rGO composite materials were produced under identical experimental conditions. The modified Marcano-Tour procedure was used to create colloidal GO. Both pure ferrite (T0 sample) and NiFe₂O₄/rGO composites were produced, with a mass ratio of 3:1 (T1 sample) and 3:2 (T2 sample). To all the resulting materials, further annealing at temperatures of 300° C, 400° C, 500° C, 600° C, and 900° C was applied [131].

Solvothermal: By using a glycol-mediated solvothermal synthesis, rGO-doped cobalt ferrite nanostructures were synthesized. In a typical CoF-rGO synthesis, 50 mg of GO was dissolved in 10 mL of di-ethylene glycol and ultrasonically processed for 6 h. Then, 40 mL of diethylene glycol (DEG) solution was combined with CoCl₂·6H₂O and FeCl₃·6H₂O in a 1:2 molar ratio, and the mixture was added dropwise to the GO solution while vigorously stirring. The earlier solution was then gradually mixed with 10 cc of the reducing solution. To make the reducing solution, 10 mL of DEG was mixed with 1g of DEG, 1g of urea, and 1g of NaOH. In a nitrogen atmosphere, the final solution, which was black in colour, was agitated for an hour. Finally, it was placed in a 100cc airtight stainless-steel autoclave and cooked at 200°C for 24 h. The product was separated using centrifugation and then dried overnight at 60°C. In the absence of GO, a similar technique was used to generate CoF nanoparticles. Later, to investigate the fictionalization impact, CoF nanoparticles were annealed at 300°C and 500°C. The samples are designated as CoF, CoF-300, CoF-500, and CoF-rGO, which

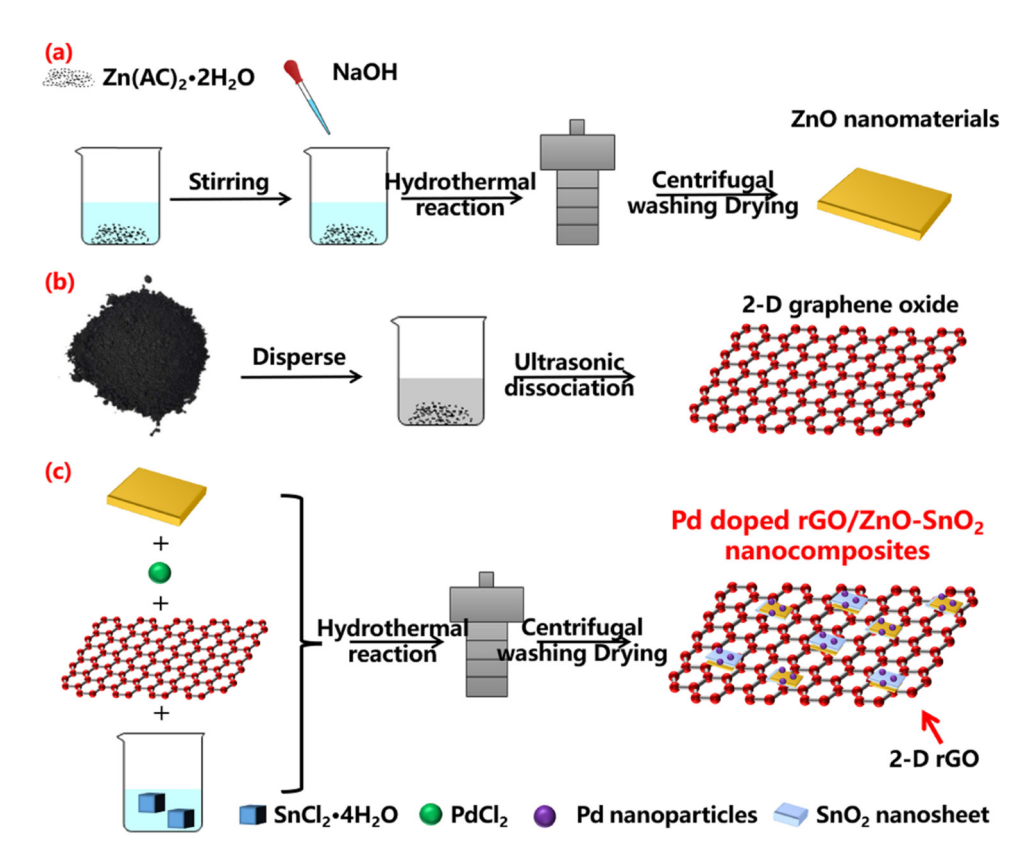


Figure 7: Hydrothermal synthesis method for rGO–ZnO. (a) Formation of ZnO nanomaterials; (b) Formation of 2D Graphine oxide; and (c) formation of hydrothermal synthesis of rGO–ZnO. Reproduced with permission from the study of Zhang et al. [132].

stand for CoFe₂O₂, annealed nanostructures, and composite nanostructures, respectively [133].

Co-precipitation: The co-precipitation of cobalt ferrite nanoparticles onto the surface of rGO particles was used to produce rGO/CoFe₂O₄. To prepare a stable suspension for this procedure, 0.126 g of dry rGO was dispersed in 100 mL of deionized water and ultrasonically processed. A mixed iron salt solution was then prepared by dissolving 0.72 g of cobalt nitrate hexahydrate and 2 g of iron nitrate nonahydrate separately in 10 mL of water. The metal solution was additionally given 0.25 g of an alcoholic cetyltrimethylammonium bromide solution. Drop by drop, ammonia solution (25%) was added to form a metal precipitate. The precipitation maintains a pH of 10-11. The addition of the rGO suspension gradually under stirring conditions was done after the metal precipitation. The reaction is kept at 80°C for 2 h. After filtering and washing with double distilled water, the solution was dried at 100°C for 10 h to achieve a neutral pH. After that, the dry material was calcined at 550°C [134].

Microwave: Graphitic carbon spinel cobalt ferrite ($CoFe_2O_2/2D-C$) composite was synthesized using a microwave combustion synthesis technique with sucrose as a template. Primarily, dissolve $0.808 \, g$ of $Fe(NO_3)\cdot 39H_2O$

(2 mmol), $0.582 \,\mathrm{g}$ of $Co(NO_3) \cdot 26H_2O$ (2 mmol) precursor, and finally 0.684 g of sucrose (C₁₂H₂₂O₁₁, 2 mmol) in a beaker with 2 mL of de-ionized water, and the mixture was being continuously stirred for 15 min with a magnetic stirrer. The corresponding solutions are subjected to rapid ultrasonication for 10 min, gentle mixing, and continuous magnetic stirring for 30 min, or until a standardized solution is produced. The 6 mL of the actual resulting solution in the beaker was placed into a preheated microwave, which was then heated to the ideal temperature of 150°C and kept for 1h. Natural convection is used to cool the beaker to room temperature, and the resulting solid product is then ground up. The triturated product was stored for 6 h in an inert gas (nitrogen) environment before being calcined in a furnace at 350°C with a constant rate of 5°C·min⁻¹. The final product was referred to as a CoFe₂O₄/ 2D-C composite (Figure 8).

One-pot synthesis method: The $CuFe_2O_4$ –rGO composite was prepared using a "one-pot" synthesis technique. Cu^{2+} and Fe^{2+} chloride salts were employed in this instance as the building blocks for $CuFe_2O_4$ -rGO composites. In this synthesis, the formation of $CuFe_2O_4$ nanoparticles and the reduction of GO resulted in the production of rGO concurrently. Here, NaOH served as both a reducing agent to

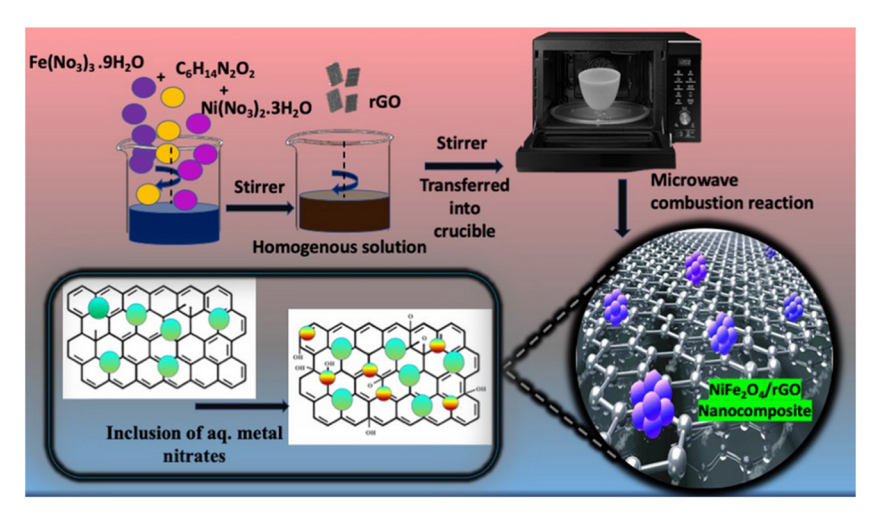


Figure 8: Microwave synthesis method for rGO-NiFe₂O₄. Reproduced with permission from the study of Mary et al. [135].

change GO into rGO and a precipitating agent for Cu²⁺ and Fe³⁺ during the production of CuFe₂O₄ nanoparticles under the circumstances of a coprecipitation process [136].

2.4 Various rGO-TMO composites for supercapacitor

2.4.1 rGO-manganese dioxide (rGO-MnO₂) composite

Recently, 3D reduced graphene oxide (rGO) is a material that can be used to solve problems with agglomeration during the reduction process. The areal capacitance of 1.13 F·cm⁻² at a greater current density of 40 mA·cm⁻². The structural electrolyte has a compressive strength of 28.5 MPa and good ionic conductivity (2.13 mS·cm⁻¹) and is made of Portland cement, KOH, and 6% poly-acrylic acid. The asymmetric structured supercapacitor outperformed

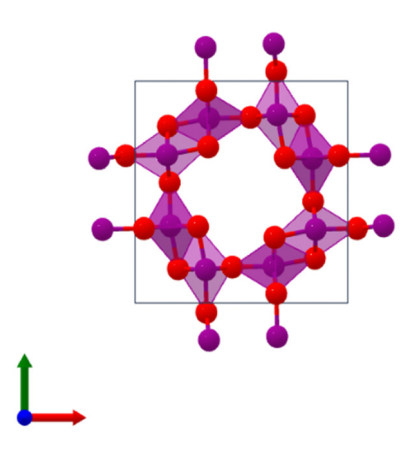


Figure 9: MnO₂ structure.

earlier research using carbon materials and resin by achieving an aerial capacitance of 51.5 mF·cm⁻² at 0.1 mA·cm⁻² rGO@MnO₂ composite supported on carbon cloth by brush electroplating. The energy density of this flexible aqueous ASC was 27.7 Wh·kg⁻¹ at a power density of 250 W·kg⁻¹ (0.9 mA·cm⁻²). The capacitor retained 76% of its capacity at a current density of 17.5 mA·cm⁻² (5 A·g⁻¹) after 10,000 charge–discharge cycles. Asymmetric supercapacitor with high flexibility using the MnO₂/rGO nanosheet-hydrogel films was used in this concept. The new polyacrylic acid sodium salt-Na₂SO₄ neutral gel electrolyte improves flexibility and performance by using bacterial cellulose (Figure 9) [137–139].

2.4.2 rGO and cobalt oxide (rGO-Co₃O₄) composites

In former research, a combination of reduced graphene oxide (rGO), cobalt oxide (Co₃O₄), and polypyrrole (PPy) to create a high-performance supercapacitor electrode. Research on supercapacitors has benefited greatly from using cobalt oxide (Co₃O₄), polypyrrole (PPy), and rGO. The largest specific capacitance values (C_{sp}) are 896 F·g⁻¹ in a 2 M KOH solution and 1,370 F·g⁻¹ in a 6 M KOH solution. Energy densities are $31.75 \text{ Wh} \cdot \text{kg}^{-1}$ for 2 M KOH and $31.43 \text{ Wh} \cdot \text{kg}^{-1}$ for 6 M KOH. The power density (P) was achieved at 11,705 W·kg⁻¹ (2 M KOH) and 11,600 W·kg⁻¹ (6 M KOH). This technology shows promise for the next generation of high-performance supercapacitors, despite some capacitance loss after 1,000 charge/ discharge cycles. The two-electrode rGO-Co₃O₄ composite electrode has a specific capacitance of 472 F·g⁻¹ at a scan rate of 2 mV·s⁻¹ in a two-electrode cell with a 2 M KOH aqueous electrolyte solution. Interestingly, even with a scan rate of 100 mV·s⁻², 82.6% of capacitance is still supported. The combination of Co₃O₄/graphene/Co₃O₄ chemically synthesized,

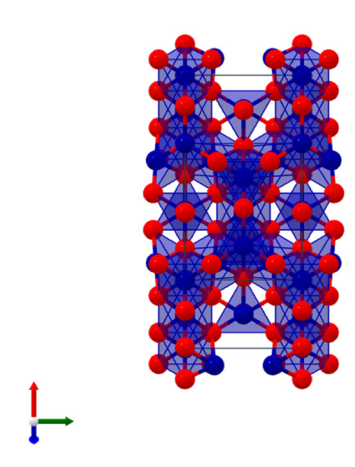


Figure 10: Co₃O₄ structure.

the performance of this composite's supercapacitance is superior: Excellent cyclic stability, a large specific capacitance, and excellent rate capability. In a 6 mol·L⁻¹ KOH solution, a needle-like nanostructure composite electrode made of $\text{Co}_3\text{O}_4/\text{rGO/NF}$ achieves a specific capacitance of 1,400 F·g⁻¹ at 1 A·g⁻¹. Its outstanding performance is a result of the material's synergistic interaction with Co_3O_4 (Figure 10) [140–142].

2.4.3 rGO-titanium dioxide (rGO-TiO₂) composite

Shape and coupling effects of rGO-TiO₂ nanocomposites for supercapacitor electrodes: researchers chemically mixed rGO with TiO₂ nanoparticles and nanobelts to create nanocomposites for supercapacitor. With rGO-TiO₂ composites, the ideal electrochemical performance is reached at a mass ratio of 3:7 for TiO₂ and rGO. Notably, the rate capability, specific capacitance, power density, and energy density of rGO-TiO₂ NBs are higher when compared to rGO-TiO₂ NPs. At a discharge current density of 0.125 A·g⁻¹, the specific capacitances of NPs (mass ratio 7:3) and rGO-TiO2 NBs are 62.8 and 225 F·g⁻¹, respectively. Due to their strength, abundance in nature, and superior mechanical properties, rGO/ TiO₂ are regarded as possible supercapacitor materials. In this system, rGO serves as the ion reservoir, accelerating the mobility of electrons during electron transfer. Mesoporous TiO₂ has more active sites and a bigger surface area, which enhances specific capacitance and cycle stability. Researchers have looked at TiO₂-C nanowire arrays covered with polyaniline (PANI) to create in situ carbon-supported titanium dioxide (ICS-TiO₂). The combination offers a continuous conductive 3D network and improves mechanical stability. Due to its broad bandgap semiconductor properties, TiO2 has been studied less for supercapacitor applications; nonetheless, it functions as a spacer with rGO to prevent rGO sheet

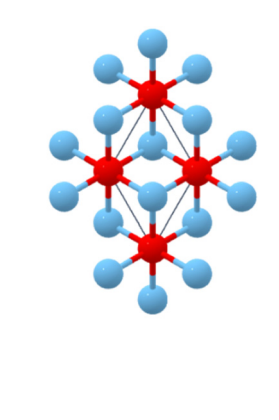


Figure 11: TiO₂ structure.

restacking. TiO_2 nanocrystals hydrogenation-induced disorder leads to an increase in electrochemical activity (Figure 11) [143–145].

2.4.4 rGO-zinc oxide (rGO-ZnO) composite

A wide-bandgap piezoelectric semiconductor called ZnO is used in UV light emitters, photodetectors, and solar cells. Its inherent point defects, such as zinc vacancies, oxygen vacancies, and interstitial sites for zinc and oxygen, are especially important in shaping its characteristics. Electron paramagnetic resonance spectroscopy can find these flaws. Hybrid nanocomposites of rGO and ZnO for supercapacitors. Researchers improved Hummer's approach and used highenergy ball milling to prepare rGO-ZnO nanocomposites. Both EDLC and pseudocapacitive contributions were present in the supercapacitors. Interestingly, after 30 cycles at $0.30 \text{ A} \cdot \text{g}^{-1}$, the capacitance retention remained at 100%. The rate capability and cycle performance are increased when graphene sheets are wrapped around ZnO nanospheres, creating highly conductive paths. At a current density of 1 A·g⁻¹, a ZnO-rGO HSC produced a specific capacitance of 1,012 F·g⁻¹. Supercapacitors made of biodegradable seaweed are another exciting advancement. These are called rGO-ZnO seaweed cellulose paper supercapacitors. These ecologically friendly, biodegradable technology products provide outstanding performance and safety (Figure 12) [146–149].

2.4.5 rGO-nickel sulphide (rGO-Ni₃S₂) composite

Using a one-step hydrothermal method, $Ni_3S_2/rGO/Ni_3S_2$ was prepared on NF. The bottom cyclic voltammetry (CV) layer was converted *in situ* from the NF substrate and the top CV layer with vertical nanosheets arose from Ni^{2+} ions

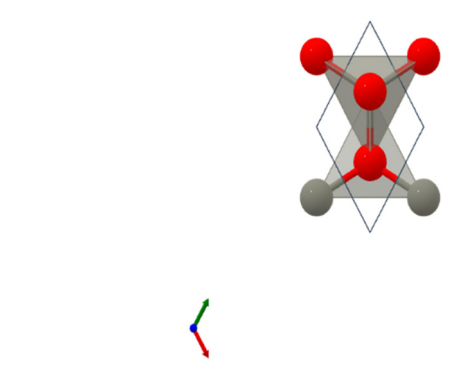


Figure 12: ZnO structure.

in the solution. It gave a specific capacitance value of $3,234.62~\mathrm{F\cdot g}^{-1}$ at a current density of $3.85~\mathrm{A\cdot g}^{-1}$. At a high rate of $100~\mathrm{mA\cdot cm}^{-2}$ after $1,000~\mathrm{cycles}$, 90% of the original capacitance was kept. Synthesis of composite 3D $\mathrm{Ni_3S_2}$ -rGO nanosheets on NF was easy. This composite has exceptional catalytic capability for the hydrogen evolution process. The rGO has an impact. The rGO affects the $\mathrm{Ni_3S_2}$ nanosheet shape, electrochemically active surface area, and quantity of active sites. $\mathrm{Ni_3S_2/MoS_2}$ on NF in Situ Morphological Evolution: For the construction of a HSC, the positive electrode is made of the hybrid material $\mathrm{Ni_3S_2/MoS_2@NF-9}$. It has an SE of $26.9~\mathrm{Wh\cdot kg}^{-1}$ at $375~\mathrm{W\cdot kg}^{-1}$ and a specific capacity of $129.2~\mathrm{C\cdot g}^{-1}$ at $0.5~\mathrm{A\cdot g}^{-1}$ (Figure 13) [150–153].

2.4.6 rGO-NiCo₂O₄ composite

N-rGO/NiCo₂O₄ nanocomposite combines nitrogen-doped rGO (N-rGO) with spinel-structured TMO (NiCo₂O₄). N-rGO/NNiCo₂O₄ has a specific capacitance of 1,078.2 $\rm F\cdot g^{-1}$ and an energy density (Ed) of 20.4 Wh·kg⁻¹. The power density is

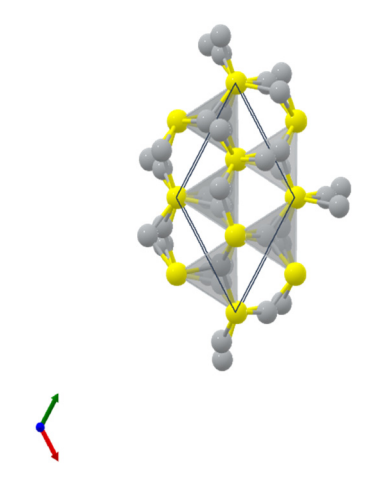


Figure 13: Ni₃S₂ structure.

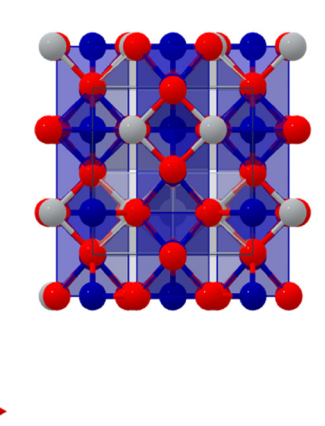


Figure 14: NiCo₂O₄ structure.

 $3,500~{\rm W\cdot kg^{-1}}$, whereas the energy density is $14.9~{\rm Wh\cdot kg^{-1}}$. Hybrid NiCo₂O₄@rGO nanostructures on NF. The hybrid electrode has a high specific capacitance of $3.6~{\rm F\cdot cm^{-2}}$ at $5~{\rm mA\cdot cm^{-2}}$ of current density (at which the capacity descends), superior cycling stability (retention of 90% after 2,000 charge/discharge cycles), and NiCo₂O₄/rGO/NiO heterostructure. ASCs made using commercial activated carbon (AC) and NiCo₂O₄/rGO exhibited the following characteristics: The energy per kilogram is $32.38~{\rm Wh\cdot kg^{-1}}$, with a total of $797~{\rm W\cdot kg^{-1}}$, excellent cycling performance, and pace ability (Figure 14) [154–156].

2.4.7 rGO-zinc cobaltite (rGO-ZnCo₂O₄) composite

Doping ZnCo₂O₄ with Ni²⁺ ions significantly improves the electrochemical performance of the material. Ni has a strong electrical conductivity, which significantly increases the specific capacitance. Ni doping results in a long life cycle as well as a strong rate ability. An ASC with Ni²⁺doped ZnCo₂O₄ and rGO in a 3.5 M KOH electrolyte has an energy density of 40 Wh·kg⁻¹. At 1 A·g⁻¹, the power density is 775 W·kg⁻¹. A flexible ASC made entirely of solid state was also created; it had a high energy density of 26 Wh·kg⁻¹ and kept 95% of its initial capacity after 10,000 cycles. The ZnCo₂O₄ @NiO//rGO architecture-based ASC device produces a maximum energy density of 46.66 Wh·kg⁻¹ at a power density of 800 W·kg⁻¹. Remarkably, the ZnCo₂O₄ @NiO//rGO architecture-based ASC device produces a maximum energy density of 46.66 Wh·kg⁻¹ at a power density of 800 W·kg⁻¹. Interestingly, the device displays 90.20% capacitance retention even after 4,000 cycles, making it a practical material with promise for energy storage applications. rGO-based mesoporous ZnCo₂O₄ nanosheet arrays: The electrochemical performance of this composite is good and has a specific capacity of 680 F·g⁻¹ at a current density of 1 A·g⁻¹. High

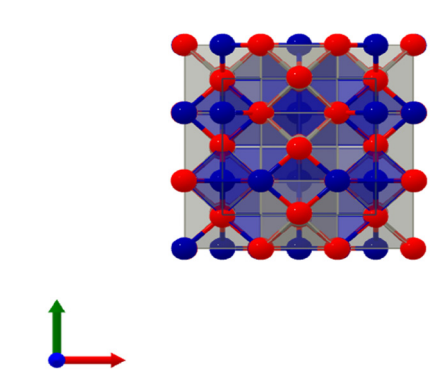


Figure 15: ZnCo₂O₄ structure.

energy density is shown by an ASC using activated porous carbon (AC) made from lotus leaves as the negative electrode and $rGO/ZnCo_2O_4$ as the positive electrode. Using freeze-dried rGO (F-rGO) as the anode and $ZnCo_2O_4$ as the cathode, an ultrahigh-energy-density ASC can reach an energy density at $0.4 \, \text{kW} \cdot \text{kg}^{-1}$ of $84.48 \, \text{Wh} \cdot \text{kg}^{-1}$ (Figure 15) [144,157,158].

2.4.8 rGO-ruthenium dioxide (rGO-RuO₂) composite

The metal oxide utilized in supercapacitor applications is RuO_2 . Excellent electrical conductivity, low resistivity, electrocatalytic activity, and thermal stability are some of RuO_2 's key properties. Fast Faradaic redox reactions are made possible by RuO_2 , which improves energy storage performance. RuO_2 and rGO work together synergistically to give specific capacitance, which is enhanced by the composite's coupled conductive network. Together, graphene (rGO) and metal oxide (RuO_2) improve energy density and cyclic stability. Good rate capability, long electrochemical cycling life (no deterioration after 2,000 cycles), and high specific capacitance (e.g. 345 $F \cdot g^{-1}$ for 15% RuO_2 loading) are

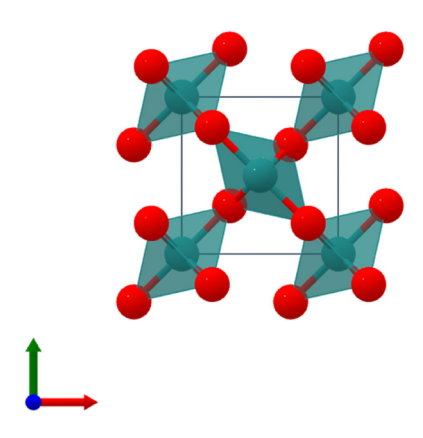


Figure 16: RuO₂ structure.

all characteristics of supercapacitors based on $rGO-RuO_2$ composites (Figure 16) [159–162].

2.4.9 rGO-CuO composite

rGO–CuO nanocomposites are created by ultrasonically synthesizing CuO nanoparticles and combining them with rGO. The qualities of CuO are electrical conductivity, low resistivity, catalytic activity, and stability at elevated temperatures. The performance of supercapacitors is improved by the synergistic actions of rGO and CuO. The rGO–CuO nanocomposite shows increased capacitance and reduced resistance. Images taken using a transmission electron microscope show CuO particles trapped in the web of rGO layers. The synergistic impact of double-layer capacitance from rGO is credited with the supercapacitor performance [163–165].

2.4.10 rGO-copper oxide (rGO-Cu₂O₃) composite

 $rGO-Cu_2O_3$ nanocomposites are created by combining ultrasonically synthesized Cu_2O_3 nanoparticles with rGO. Supercapacitor performance is improved by the synergistic actions of rGO and Cu_2O_3 . The $rGO-Cu_2O_3$ nanocomposite shows greater capacitance and less resistance. The supercapacitor was created utilizing $rGO-Cu_2O_3$ nanocomposite electrodes, and its specific capacitance is about $137 \ F \cdot g^{-1}$ (Figure 17) [166–169].

2.4.11 rGO-vanadium pentoxide (rGO-V₂O₅) composite

Sol–gel synthesis has been used by researchers to produce rGO-anchored vanadium pentoxide (V_2O_5) nanorods. These materials' electrochemical analysis reveal the following fascinating characteristics: At a scan rate of 10 mV·s⁻¹, the

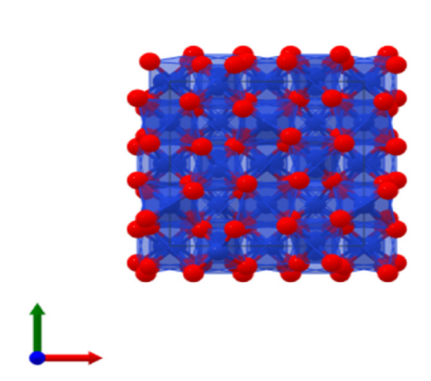


Figure 17: Cu₂O₃ structure.

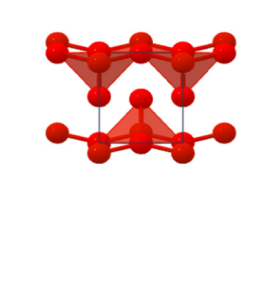


Figure 18: V₂O₅ structure.

large surface area of V_2O_5 electrode material results in a high specific capacitance of $112\,\mathrm{F}\cdot\mathrm{g}^{-1}$. The $\mathrm{rGO/V_2O_5}$ electrode material has a higher specific capacitance value than pure V_2O_5 , measuring $218.4\,\mathrm{F}\cdot\mathrm{g}^{-1}$ at $10\,\mathrm{mV}\cdot\mathrm{s}^{-1}$. rGO nanosheets are thought to be responsible for this improvement. Adding GO to V_2O_5 improves the nanocomposite's electrochemical performance significantly. These composites have a high specific capacitance of $438.1\,\mathrm{F}\cdot\mathrm{g}^{-1}$ at a current density of $1\,\mathrm{A}\cdot\mathrm{g}^{-1}$. Researchers developed electrode materials based on 2D heterostructures of rGO and V_2O_5 nanosheets (V_2O_5 NS) for ASC applications. These heterostructures have a specific capacitance of $253\,\mathrm{F}\cdot\mathrm{g}^{-1}$ at a current density of $1\,\mathrm{A}\cdot\mathrm{g}^{-1}$. When combined with rGO, the capacitance dramatically increases to $635\,\mathrm{F}\cdot\mathrm{g}^{-1}$, which is 2.5 times higher (Figure 18) [170–172].

2.4.12 Various other composites

The characteristics and performances of MnO_2 –NiO–ZnO @GO electrodes are affected by 8.0 MeV C^{2+} ion radiations. Electrochemical investigations revealed that electrodes with radiation dosages of 5.0 × 1,015 yielded specific capacitances with the value of 1,627, and 7.5 × 1,015 ions·cm⁻² yielded specific capacitances with the value of 1,960 F·g⁻¹ [173].

A study found that the mass loading (thickness) of rGO film electrodes affects the electrochemical performance. Due to their substantial specific surface area and consistent pore distribution, these rGO film electrodes with a mass loading of 6.7 $\rm mg\cdot cm^{-2}$ display a high specific capacitance of 173.4 $\rm F\cdot g^{-1}$ (1.16 $\rm F\cdot cm^{-2})$ at $1\,\rm A\cdot g^{-1}$. The supercapacitor constructed with the prepared rGO film electrode exhibits outstanding cycling stability after 10,000 cycles, with 85.6% retention, a high area capacitance of 1.03 $\rm F\cdot cm^{-2}$, a large SE of 0.073 mWh cm², and an SP of 3.3 mW·cm². This rGO film may be a suitable electrode material for use in supercapacitors based on its outstanding performance [174].

A thin film of GO was produced on the indium thin oxide substrate using the spin-coating process, with GO in

various concentrations that were distributed in water. The oxygen in the GO film was removed using thermal reduction, which took place at 200°C for 1 h. A scan rate of $25 \text{ mV} \cdot \text{s}^{-1}$ was used to measure the thinnest rGO film with the highest specific capacitance of $6.53 \text{ F} \cdot \text{g}^{-1}$ [175].

The powders made using urea as a precipitant (NFO-U) and sodium acetate (NFO-C) displayed a nanoparticle structure and a nanosheet form. The crystallinity of the two NFOs was excellent, at $1\,\mathrm{A\cdot g^{-1}}$, and the specific capacity of NFO-U is 240.9 $\mathrm{F\cdot g^{-1}}$ which increases to 128% after 2,000 cycles [176].

A low-cost approach for producing nickel ferrite nanostructures as an alternative TMO electrode material for clean energy. At $2\,\mathrm{mV}\cdot\mathrm{s}^{-1}$ scan rate, the maximum specific capacitance attained by NiFe₂O₄ electrode material was $541\,\mathrm{F}\cdot\mathrm{g}^{-1}$ without the use of heterostructures, template-based techniques, or any carbon-based materials [177].

A regulated number of functional groups containing oxygen on few-layered GO graphene oxide sheets and metallic Zn atoms undergoes a redox process. The ZnFe₂O₄/ rGO at a high current rate of $1.0\,\mathrm{A\cdot g^{-1}}$ shows a reversible capacity of $1,022\,\mathrm{mA\cdot h^{-1}.g^{-1}}$ for 500 continuous cycles [178].

A 3D core–shell $ZnFe_2O_4/NiMoO_4$ nanosheet was studied for supercapacitor applications by fabricating $ZnFe_2O_4$ nanosheet arrays on conductive NF substrates embellished with rGO. At a power density of 799 W·kg⁻¹, prolonged cyclic durability (89.6% after 7,000 cycles) and a high energy density of 58.6 Wh·kg⁻¹, an ASC device made of ZFO@NMO NSAs@rGO-NF as the MOF-derived hollow porous carbon acting as the anode and cathode showed its potential use in advanced HSCs [179].

A one-step coprecipitation method was used on a binary compound comprising rGO and doped iron oxide (rGO/MeFe₂O₄), with sodium hydro-oxide serving as a GO reducing agent. The rGO/MnFe₂O₄ composite electrode showed an aerial capacitance of 232 mF·cm⁻² at a scan rate of $5\,\text{mV·s}^{-1}$ and a gravimetric capacitance of $147\,\text{F·g}^{-1}$. The (rGO/MnFe₂O₄/Ppy) electrode significantly improved in the final phase, reaching 232 F·g⁻¹ and 395 mF·cm⁻², respectively, due to the synergistic effect of Ppy additions [180].

The application of rGO impregnated with Al^{3+} – (Mn)/(Cu) ferrite as electrode materials for super-capacitor applications and photo-electrocatalytic water splitting. The pseudocapacitance and EDLC characteristics were found with specific capacities of $216 \, \mathrm{F} \cdot \mathrm{g}^{-1}$ for manganese and $142 \, \mathrm{F} \cdot \mathrm{g}^{-1}$ for copper. The two-electrode device demonstrated 99.1% capacity retention after 5,000 cycles [181].

The effective hydrothermal production of MnFe₂O₄/PEDOT/rGO, poly(3,4-ethylenedioxythiophene), and manganese ferrite. At $1 \, \text{A} \cdot \text{g}^{-1}$ current density, the specific capacitance values to 298.97 F·g⁻¹, and at $2 \, \text{mV} \cdot \text{s}^{-1}$ scan rate, the

specific capacitance values to $325~\rm F\cdot g^{-1}$. At a greater current density of $10~\rm A\cdot g^{-1}$, the capacitance retention of $87~\rm F\cdot g^{-1}$ was observed. The substance showed excellent electrochemical stability, keeping 81% of its capacitance even after 5,000 cycles [182]. The addition of PEDOT impacts the specific capacitance and electrochemical stability of composite electrodes by improving charge storage capacity, enhancing charge transfer kinetics, and increasing overall electrochemical stability, leading to improved performance of supercapacitors. As a conductive polymer, poly(3,4-ethylene-dioxythiophene) (PEDOT) is renowned for its exceptional electrical properties, which include high conductivity and stability. The electrochemical efficacy of supercapacitors can be substantially impacted by the incorporation of PEDOT into composite electrodes.

PEDOT leads to an increase in specific capacitance, principally through its pseudocapacitive behaviour. The electrode–electrolyte interface undergoes rapid and reversible faradaic redox reactions, resulting in charge storage that exceeds the electric double-layer capacitance (EDLC) of materials such as rGO or TMOs. This phenomenon is referred to as pseudocapacitance.

The overall charge storage capacity of the electrode material is enhanced by the incorporation of additional charge transfer pathways due to the redox-active nature of PEDOT. In comparison to composite electrodes lacking PEDOT, this results in an elevated specific capacitance.

Efficient electron transport within the electrode material is also facilitated by the conductive character of PEDOT, which further enhances its charge storage capacity.

As far as the enhancement of electrochemical stability is concerned, PEDOT inhibits the agglomeration or restacking of active material particulates, including rGO or TMOs, during charge—discharge cycles by acting as a stabilizing agent within the composite electrode structure.

This leads to enhanced electrochemical stability by preventing the loss of active surface area as well as ensuring the electrode structure's integrity over multiple cycles.

In addition, the electrode material's resilience under severe electrochemical conditions is ensured by PEDOT's chemical stability, which reduces degradation and extends the supercapacitor's operational lifespan.

In addition to the double-layer capacitance, the inclusion of PEDOT on the electrode surface introduces additional redox-active sites, which promote pseudocapacitive charge storage mechanisms.

The conductive polymer matrix of PEDOT enables the efficient transport of charge and electrons within the electrode material, thereby enhancing charge—discharge kinetics and reducing internal resistance.

The overall electrochemical stability of the composite electrode is enhanced by the chemical stability and compatibility of PEDOT with the electrolyte, which reduces the probability of degradation mechanisms including active material dissolution or electrolyte decomposition.

Furthermore, glycol-functionalized cobalt ferrite nanoparticles and cobalt ferrite composites with rGO for usage as the supercapacitor electrodes were synthesized using a onepot solvothermal technique. The cobalt ferrite composites with rGO demonstrated at a scan rate of $2\,\mathrm{mV\cdot s^{-1}}$, 8% capacitance retention after 2,000 cycles, and high specific capacitance of $551\,\mathrm{F\cdot g^{-1}}$ [183].

They used a hydrothermal technique to synthesize a three-dimensional hierarchical electrode material made of nickel ferric oxide and rGO nanostructures. The NiFe₂O₄/r-GO nanostructured electrode with a current density of $0.65~\rm A\cdot g^{-1}$ has a specific capacity of $362.46~\rm F\cdot g^{-1}$. It has a power density of $276.22~\rm kW\cdot kg^{-1}$ and a high energy density of $36.37~\rm Wh\cdot kg^{-1}$, the composite exhibits enhanced cycling stability over 2,000 cycles with no capacitance reduction [184].

A hybrid of rGO and NiFe $_2$ O $_4$ nanocomposite and nickel ferrite nanoparticles (NFN) is used to produce the nanoparticles. This electrode may be an alluring choice for supercapacitor applications because of its high capacitance of 584.63 F·g $^{-1}$ and 91% retention after 2,000 consecutive cycles [185].

NiFe₂O₄/rGO composite material is formed by reducing graphene oxide (rGO) and decorating it with NiFe₂O₄ nanoparticles. SC device with electrodes consisting of both natural gas and AC, which demonstrated outstanding cycle stability, high specific capacity, and power and energy densities of 75 Wh·kg⁻¹ and 2,343 W·kg⁻¹, respectively [186,187].

 $NiFe_2O_4$ -NiCo-LDH@rGO composite material has high electrical conductivity and can transport and disperse ions. The electrode formed of this composite material is very durable and has a high specific capacitance of 750 C·g⁻¹ [188].

To form hierarchical functional composites, NiO and NiFe₂O₄ nanoparticles are layered on top of rGO nanoflakes derived from coconut coir biowaste. To form hierarchical functional composites, NiO and NiFe₂O₄ nanoparticles are layered on top of rGO nano-flakes derived from coconut coir biowaste, keeping current severe electrochemical conditions is ensured by PEDOT's density of $1\,\mathrm{A}\cdot\mathrm{g}^{-1}$ with a high specific capacitance of 599.9 F·g⁻¹ having a retention rate of 86.5% were achieved even after 2,000 cycles to the synergies created by the combination of NiFe₂O₄ nanoparticles and rGO nanoflakes. The composite also show an excellent 96.5% photocatalytic degradation efficiency when activated by visible light [189].

According to the researchers, after 10,000 cycles, the rGO-NiFe₂O₄ hybrid demonstrated improved cycle

stability and no significant capacity loss. At 0.5 A·g⁻¹, the hybrid provided a higher specific capacitance value of 215.7 F·g⁻¹ [190].

NiFe₂O₄ nano-cubes and rGO cryogen electrodes were used to create a flexible solid-state capacitor with a voltage of 1.8 V. The combination nickel ferrite with rGO electrode displayed at a constant current density valued to 1 A·g⁻¹ a high charge storage capacity valued to 488 F·g⁻¹, excellent rate ability, with initial capacitance value after 10,000 cycles with cycling performance 89.8%, as a result of the synergistic effects between graphene nanosheets and NFNs [191].

The nickel ferrite graphene nanosheet composite increased specific capacitance by twofold (264 F·g⁻¹) and threefold (845 F·g⁻¹). Furthermore, the NiFe-A@GNS electrode retained 94.3% of its capacity after 5,000 cycles, outperforming the NiFe₂O₄ electrode's retention rate of 62% after 2,000 cycles). At a current density of 1.0 A·g⁻¹, the nickel ferrite graphene nanosheet composite has a high power density of 620 W·kg⁻¹ and a high energy density of 30.8 Wh·kg⁻¹ [192].

A freestanding nickel ferrite electrode nanosheet was produced and deposited on the three-dimensional NF termed NiFe₂O₄/NF using a simple hydrothermal technique. The formation of nickel ferrite electrode nanosheets on the three-dimensional NF electrode demonstrated at a current density of 1 A·g⁻¹, a comparatively high capacitance of 975 $F \cdot g^{-1}$, excellent capacitance retention from 1 to 10 $A \cdot g^{-1}$ range at the rate valued to rate capability 74.6% and excellent cycle life at 10 A·g⁻¹ after 3,000 charge-discharge cycles about 95% capacitance retention [193].

The NiFe₂O₄ nanoparticle and NiFe₂O₄/CNT composite were examined by the researchers using a number of analytical methods. The retention rate was observed 89.16% after 5,000 cycles, the nickel ferrite and carbon nanotube composite- modified single electrode displayed 343 F·g⁻¹ (GCD) and a specific capacitance value of 670 F·g⁻¹ (CV), respectively. Additionally, a two-electrode device with an AC anode and a cathode constructed of spinel NiFe₂O₄/CNT composite had a specific capacitance of 85.93 F·g⁻¹ (GCD) and 118.36 F·g⁻¹ (CV), respectively, and a power density value of 466.66 W·kg⁻¹ opposed by an energy density value of 23.39 Wh·kg⁻¹ [194].

rGO-CoF (cobalt ferrite)-based electrodes were used. A one-pot solvothermal synthesis of glycol-functionalized CoF nanoparticles and the composite with rGO for the supercapacitor electrode was carried out in this study, and CoF-rGO displays a high specific capacity of 551 F·g⁻¹, 98% capacitance retention after 2,000 cycles at a scan rate of 2 mV·s⁻¹ [195].

Flower-like, rod-shaped, and spherical nanostructured ternary composites comprising GO, PANI, ZnFe₂O₄ nanoparticles are synthesized and employed as a hybrid SC, with the energy density (45.18 Wh·kg⁻¹), power density (302.73 W·kg⁻¹), highest specific capacitance (594 F·g⁻¹), and cycle stability after 1,500 cycles. These results showed the PANI/GO/ZFS hybrid electrodes' enormous potential as powerful supercapacitors for a range of uses, from electrical gadgets to transportation [196].

A hybrid ZnFe₂O₄ nanorod and ZnFe₂O₄ nanorod rGO structure based on iron and zinc was experimentally studied. The specific capacitance of ZnFe₂O₄-rGO was calculated to be 1,419 F·g⁻¹ with a cyclic stability of 93% after 5,000 consecutive voltammetry cycles at a scan rate of 10 mV·s⁻¹ [197].

Zinc ferrite (ZnFe₂O₄) and graphene nanosheets are synthesized and characterized for use in supercapacitors. The ZnFe₂O₄/graphene nanosheet electrodes' performance in devices was determined at a 5 mV·s⁻¹ scan rate with an estimated specific capacitance of 789.2 F·g⁻¹, and the device demonstrated exceptional capacitive performance [198].

CuFe₂O₄/rGO as electrode materials for HSCs is shown here using a simple microwave method. The appealing CG composite at a 2 A·g⁻¹ current density had a higher specific capacity of 800 C·g⁻¹ and superior cycle stability because ferrite nanoparticles were uniformly inserted into rGO sheets to create a nanostructure. It is an HSC device with an SP of 455 W·kg⁻¹ and an SE of 18.3 Wh·kg⁻¹ and exhibits exceptional electrochemical performance. It is notable that the cyclic stability is outstanding, demonstrating the superiority of CG electrodes with a capacity retention after 3,000 cycles of 98% [199].

There are various factors to consider while selecting the optimum electrode materials for supercapacitors. These include excellent conductivity, chemical inertness, mechanical stability, compatibility with the electrolyte, and compatibility with the current collector [183,194,200]. In rGO-MnO₂, MnO₂ has an excellent specific capacitance and is a typical pseudocapacitive material. High electrical conductivity is provided by rGO [189,201,202]. This mixture could provide a balance between power density and energy density. rGO-Co₃O₄, another pseudocapacitive substance is Co₃O₄ [203-205]. This combination can offer good capacitance performance. rGO-TiO2, because of its stability and large surface area, TiO2 is often utilized in supercapacitors. RuO₂ has a high specific capacitance, which is well known [206-208]. In terms of energy storage, this combination may be exceptional. rGO-Cu₂O₃, although less frequent, Cu₂O₃ has been researched for use in supercapacitors [209-211]. Although less common, this combo has potential. $rGO-V_2O_5$, the pseudo capacitance of V_2O_5 is excellent. Charge transport is improved by rGO. For some applications, this combination can be intriguing [180,212,213]. rGO-ZnO, it is possible that this combo will perform mediocrely. rGO-Ni₃S₂, a potential material for pseudocapacitors is Ni₃S₂ [214–216]. This combination could have effective energy-storage capabilities. rGO-NiCo2O4, a mixed metal oxide with high pseudocapacitance is NiCo₂O₄. This combination could result in performance that is balanced [217–219]. A rGO–ZnCo₂O₄, performance from this combo may be respectable [220–222]. A rGO–RuO₂, due to its high specific capacitance, RuO₂RuO₂ is well recognized [223–225]. When it comes to energy storage, this mixture could be exceptional [226–228]. Keeping in mind that the exact requirements of your supercapacitor, such as energy density, power density, and cycle stability, will determine the choice of electrode material [229–231]. Further investigation and experimentation are necessary to choose the ideal combination depending on our application demands, because each material has advantages and limits [232–234].

2.5 Composites of BMO and metal oxide

Figure 19a shows X-ray diffraction (XRD) examination of NiFe₂O₄/rGO nanoparticles, which are estimated to be

about 20 nm in size. Figure 19b shows $NiFe_2O_4$ nanoparticles are evenly distributed across the surface of rGO plates. $NiFe_2O_4$ and $NiFe_2O_4/rGO$ CV in 0.1 M KOH solution at the potential range of 0 to 500 mV is shown in Figure 19c. Both graphs show a redox peak. The addition of rGO to the structure of $NiFe_2O_4$ redox peaks, increases the current density, and reduces the overpotential in the graphene-containing electrode, validating the improvement in electrode conductivity. The peaks become sharper as the scan rate increases. Figure 19d shows that the peak potential tends to positive values with increasing scan rate, suggesting that the reaction is quasi-reversible [235].

The XRD and scanning electron microscopy (SEM) images of the $CoFe_2O_4$ -rGO (CoF-rGO) nanocomposite are shown in Figure 20a and b. Figure 20c shows the CoF-rGO nanocomposites in an alkaline (2 M KOH) electrolyte demonstrating improved electrochemical behaviour. At a scan rate of 2 mV·s⁻¹, CoF-rGO displays a high C S of 551 F·g⁻¹ and retains 98% capacitance retention after 2,000 cycles. The

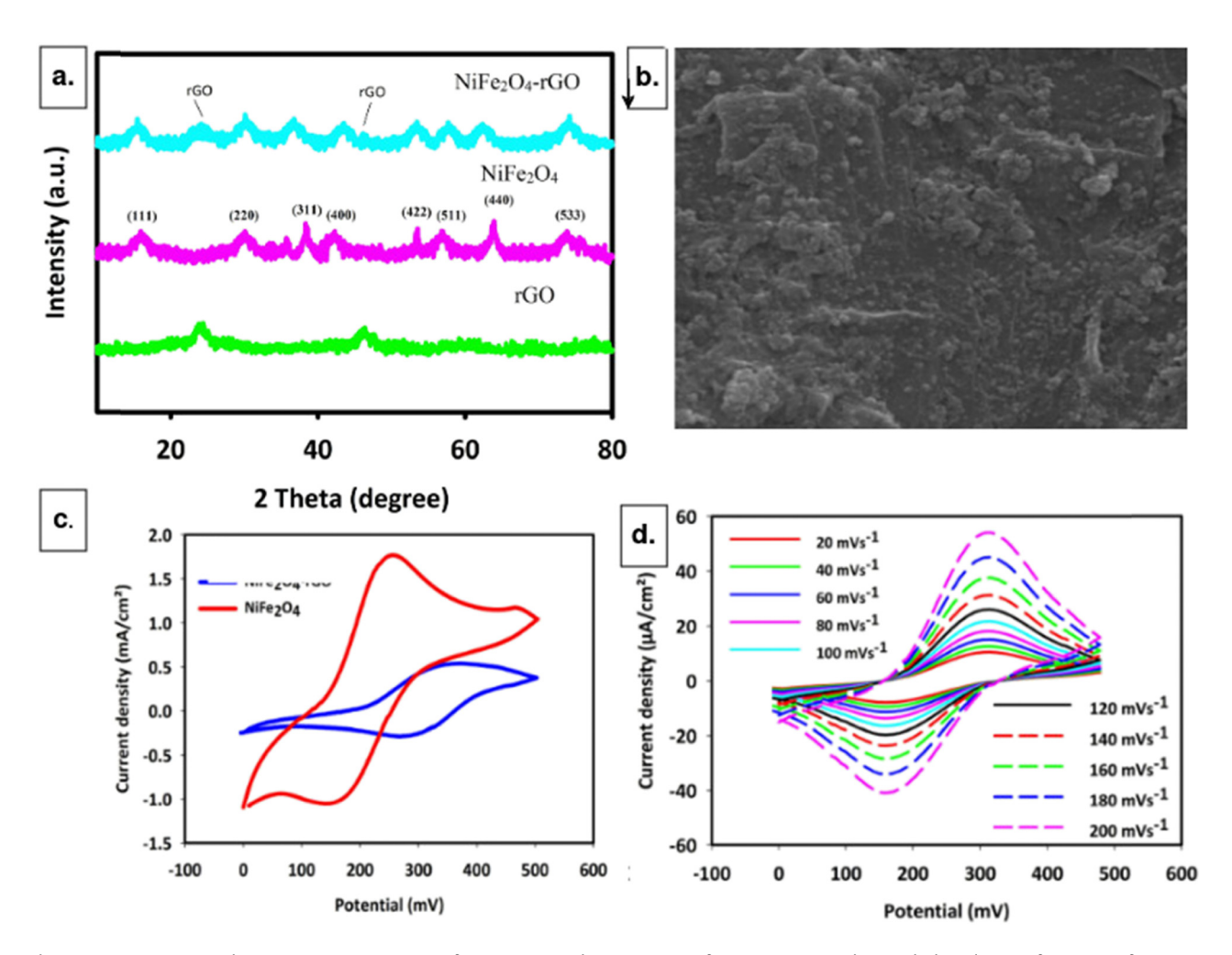


Figure 19: (a) Scanning electron microscopy image of NiFe₂O₄/rGO, (b) XRD image of NiFe₂O₄/rGO, and (c) and (d) cycling performance of NiFe₂O₄/rGO. Reproduced with permission from the study of Askari et al. [235].

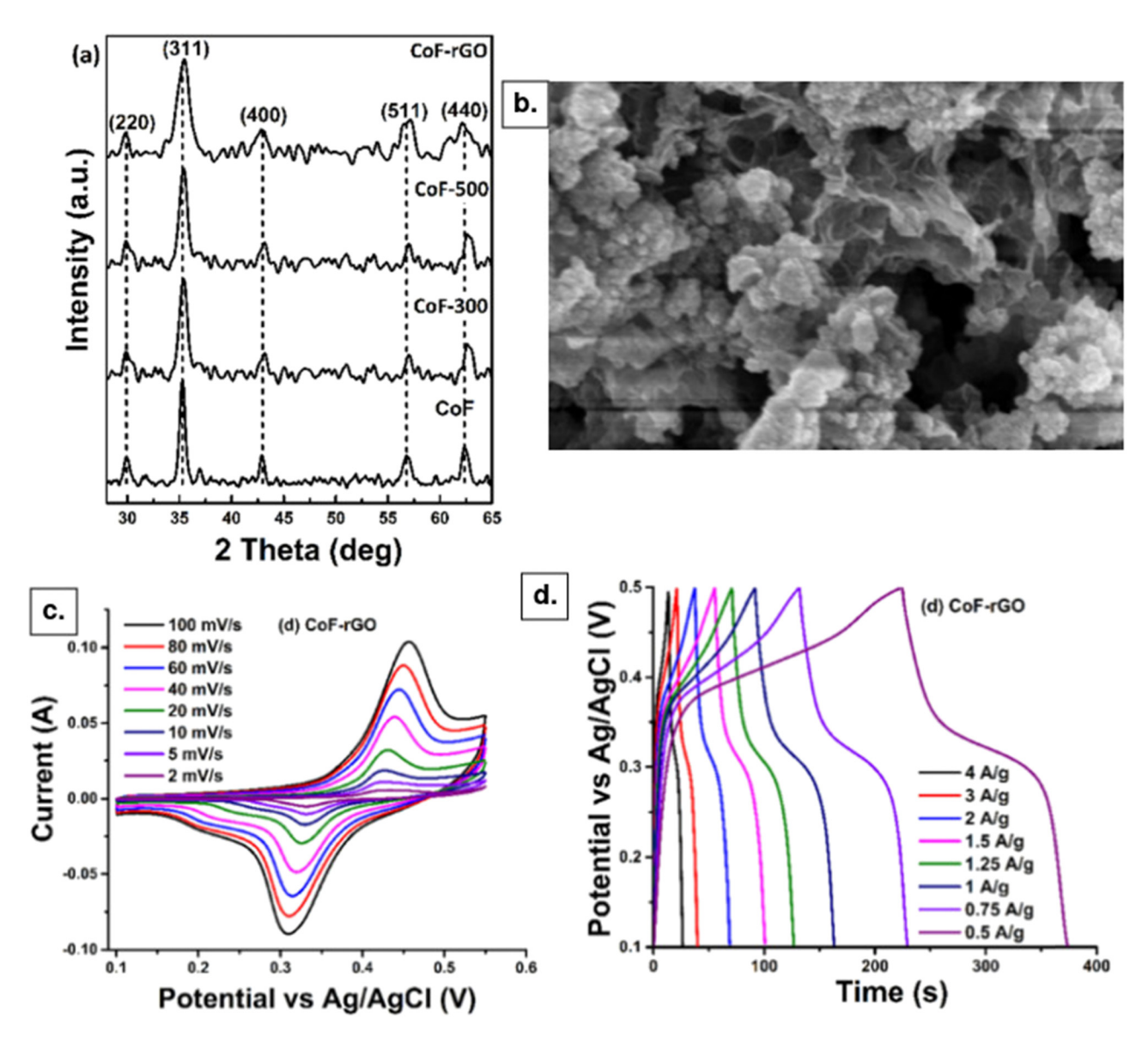


Figure 20: (a) XRD image of CoFe₂O₄-rGO, (b) SEM image of CoFe₂O₄-rGO, (c) cycling performance of CoFe₂O₄-rGO, and (d) charge–discharge behaviours of CoFe₂O₄-rGO composites at a current density of 0.5 A· q^{-1} . Reproduced with permission from the study of Rani and Sahu [180].

relationship between current densities and corresponding capacitance values is shown in Figure 6d. rGO makes it clear that as current densities increase, the capacitance values decrease. The longer charge–discharge time for CoF-rGO is shown in Figure 20d, indicating a somewhat higher capacitance of the composite as compared to the as-prepared and annealed CoF. The CoF-rGO composite exhibits a noteworthy C S of 187 $\text{F} \cdot \text{g}^{-1}$ at a current density of 0.5 $\text{A} \cdot \text{g}^{-1}$ [180].

Figure 21a shows $NiCo_2O_4/rGO$ and $NiCo_2O_4$ X-ray diffractometer patterns. Figure 21b shows the SEM image of $NiCo_2O_4/rGO$, through *in situ* development, the $NiCo_2O_4$ not only has good mechanical qualities, but it also resists falling off while charging and discharging. Ion diffusion

in the gaps is aided by NiCo₂O₄/rGO. rGO primarily serves as a supporting and conducting component in the composite mode of rGO and NiCo₂O₄, while the pseudocapacitance performance of the NiCo₂O₄ spinel structure is shown in Figure 21c. The composite material's electrochemical performance is enhanced due to the equally dispersed NiCo₂O₄/rGO needles, more moderate gap, broad contact area with the electrolyte, shorter ion transmission channel, and so on. In the curve created using the solvothermal approach, there are two pairs of redox peaks. It may have to do with changing the equivalent states of $\text{Co}^{2+}/\text{Co}^{3+}/\text{Co}^{4+}$ and $\text{Ni}^{2+}/\text{Ni}^{3+}/\text{Ni}^{4+}$, suggesting that the primary mechanism for storing energy is the presence of pseudocapacitance (Figure 21d).

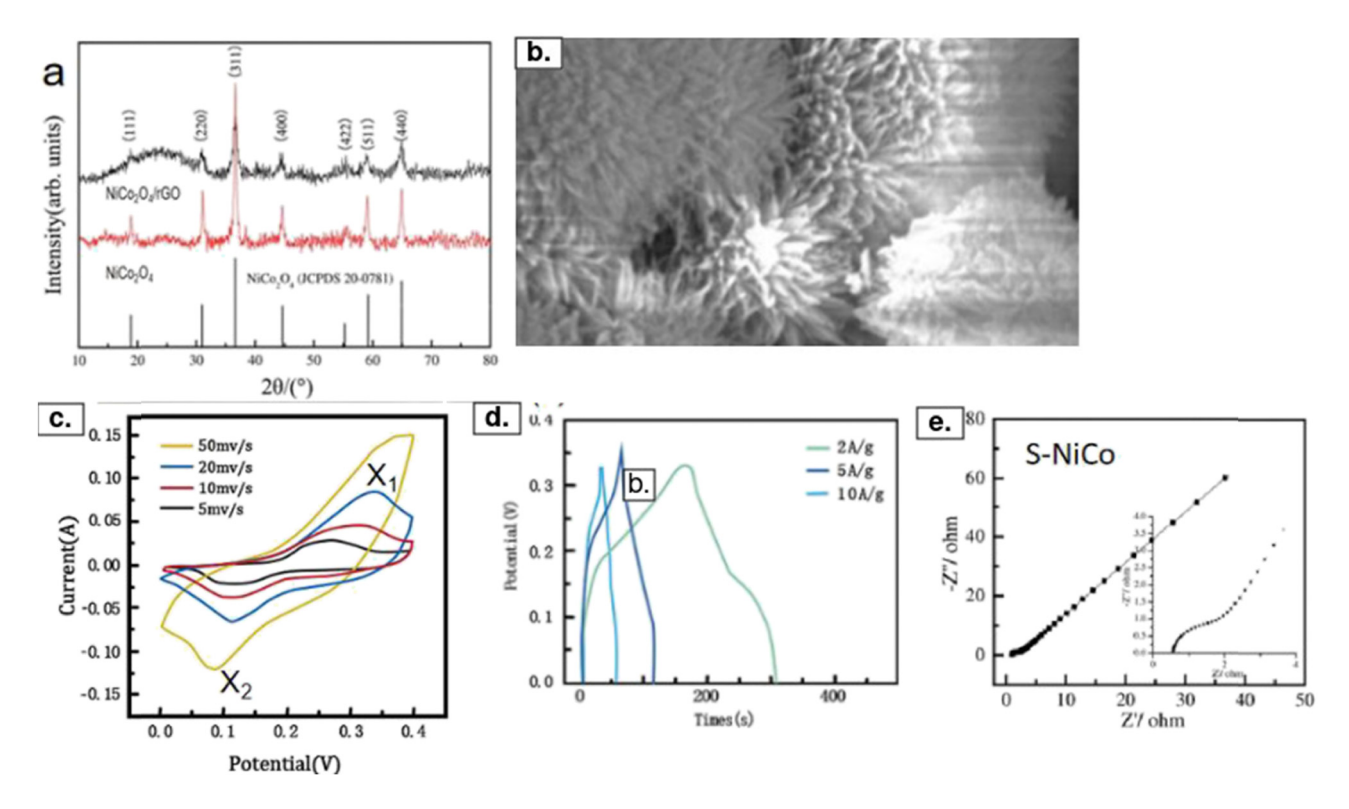


Figure 21: (a) XRD image of $CoFe_2O_4$ -rGO, (b) SEM image of $CoFe_2O_4$ -rGO, (c) cycling performance of $CoFe_2O_4$ -rGO, and (d) charge–discharge behaviours of $CoFe_2O_4$ -rGO composites at a current density of $0.5 \text{ A} \cdot \text{g}^{-1}$. (e) Nyquist plots (EIS) of the $NiCo_2O_4$ /rGO. Reproduced with permission from the study of Yao et al. [236].

NiCo₂O₄/rGO produced by solvothermal technique has a specific capacitance of 935.6 $\text{F}\cdot\text{g}^{-1}$, as determined by a constant current charge–discharge test conducted at $2\,\text{A}\cdot\text{g}^{-1}$. Figure 21e shows the two materials' AC impedance diagrams are composed of a low-frequency linear line and a high-frequency Nyquist curve. NiCo₂O₄/rGO has a resistance of 1.35 Ω . However, it has been shown that there is good electrode-to-electrolyte contact. The NiCo₂O₄/rGO material electrode made using the two techniques has a reasonably low resistance, suggesting that the addition of GO may lower the electrode's resistance and hence its resistance to ion migration [236].

According to the aforementioned findings, combining two different kinds of materials improves the composite material's redox capacity while also improving its structural stability. Above all, rGO-BMOs' enhanced conductivity may operate as a structural support for active electrode materials, facilitating an efficient electrical connection that can maximize the combined effects of each component. These factors make it crucial for supercapacitors to adjust the microstructure, crystallinity, and electrical conductivity of oxide-based materials.

Table 2 lists various composites of carbon, BMO, and their combinations with their synthesis process with specific

capacitance, current density, and stability of electrode for supercapacitor performances [237–239]. The comparison in the table shows how rGO with BMO enhances charge storage capability [240–242]. We can see that when combined with Ni, Mn, and Co, it gives a higher specific capacitance than when given alone [201,243,244].

3 Limitations of the current study

- a. Power density trade-off vs energy density: To achieve a balance between power density and energy density is one of the primary obstacles [245–247]. Despite the fact that materials such as rGO and a variety of metal oxides possess high power density as a result of their rapid charge–discharge capabilities, it remains difficult to achieve a comparable energy density [248–250].
- b. Cycle stability and longevity: Despite optimistic advancements, the maintenance of long-term cycle consistency and durability continues to be a substantial challenge [189,251,252]. The capacitance degradation of numerous supercapacitor electrodes, including rGO-metal oxide composites, over extended charge-discharge cycles is

 Table 2: Electrochemical analysis of various composite electrodes

Material	syntnesis process	Specific capacitance	current	Energy density Power density		Stability	Stall late	kelerences
rGO film		173.4 F·g ⁻¹	1 A·g ⁻¹			85.6% retention after 10,000		[183]
rGO	Hummers	274 F·g ⁻¹				cycles		[194]
rGO	Hummers	461 F·g ⁻¹	0.75 A·g ⁻¹			1,000 cycles	200 mV·s ⁻¹	[194]
NiFe ₂ O ₄ /NiCo ₂ O ₄ /GO		14,70 F·g ⁻¹	1 A·g ⁻¹			89.9% after 3,000 cycles		[194]
NiCo ₂ S ₄ /rGO	hydrothermal	1,072 F·g ⁻¹	1 A·g ⁻¹	41.52 Wh·kg ⁻¹	1,067 W·kg ⁻¹	82% after 3,000 cycles		[200]
NiTe ₂ -Co ₂ Te ₂ @rGO	hydrothermal	223.6 mA·h ⁻¹ ·g ⁻¹	1.0 A·g ⁻¹	51 Wh·kg ⁻¹	800 W·kg ⁻¹	89.3% after 3,000 cycles		[200]
MnNi ₂ O ₄ /rGO		575 F·g ⁻¹	$0.5 \text{ A}\cdot\text{g}^{-1}$			93% after 2,000 cycles		[200]
NiMoO ₄ /rGO	hydrothermal	1,400 F·g ⁻¹	20 A·g ^{−1}			91% after 2,000 cycles		[201]
Ag₂WO ₄ /rGO	Sonochemical	534 F·g ⁻¹		68 Wh·kg⁻¹		102.1% after 5,000 cycles	5 mV·s ⁻¹	[202]
CeO ₂ -SnO ₂ /rGO	hydrothermal	156 F·g ⁻¹	0.5 A·g ^{−1}					[189]
CZSrG		992 F·g ⁻¹		$2.05\mathrm{Wh\cdot kg}^{-1}$	1,800 WmA·kg ⁻¹		10 mV·s ⁻¹	[203]
CuO/Mn ₃ O ₄ /rGO		856 F·g ⁻¹				82% after 2,000 cycles)		[204]
PPy/rG0	chemical polymerization	9,300 mF·cm ⁻²		167 µWh kg ⁻¹		94.47% after 10 000 cycles		[205]
Co ₃ O ₄ /rGO	hydrothermal	754 F·g ⁻¹				96% after 1,000 continuous		[206]
						cycles		
$Cu_2O/MoS_2/rGO$	microwave	388 F.g ⁻¹				95.6% after 3,000 cycles		[207]
Ni-Co LDH/rGO		2,987 F·g ⁻¹	1 A·g ⁻¹	39.9 Wh·kg ⁻¹	1.48 kWkg ⁻¹			[208]
MoO ₃ /rGO		486 F·g ⁻¹	1 A·g ⁻¹			92% after 1,000 cycles		[209]
Fe ₃ O ₄ /rG0		416 F·g ⁻¹	5 A·g ⁻¹			88.57% after 1,000 cycles		[210]
W ₁₈ O ₄₉ NWs-rGO		365.5 F·g ⁻¹	1 A·g ⁻¹	28.5 Wh·kg ⁻¹	751 Wkg ⁻¹	96.7% after 12,000 cycles		[211]
NiMoO ₄ /3D-rGO		932 F·g ⁻¹		32.36 Wh·kg ⁻¹	17.5kWkg ⁻¹			[180]
FeNiS/rGO		2,454 F·g ⁻¹	1 A·g ⁻¹	64.3 Wh·kg ⁻¹				[212]
PPY-TiO ₂ -rGO		1,171 F·g ⁻¹			$799.74~{ m Wkg}^{-1}$			[213]
NiFe ₂ O ₄ /rGO		1,320 C·g ⁻¹	1 A·g ⁻¹	$75~\mathrm{Wh~kg}^{-1}$	2,343 W kg ⁻¹	98% after 5,000 cycles		[214]
CoF-rGO		551 F·g ⁻¹				98% after 2,000 cycles	2 mV·s ⁻¹	[215]
NiFe ₂ O ₄ /rGO		599.9 F·g ⁻¹	1 A·g ⁻¹			86.5% after 2,000 cycles		[216]
NiFe ₂ O ₄ /rGO	hydrothermal					98% after 5,000 cycles		[217]
CoFe ₂ O₄/rGO		1,032 F·g ⁻¹	3 A·g⁻¹	65.8 Wh·kg ⁻¹	1,500 W·kg ⁻¹	96% after 5,000 cycles		[218]
PANI/NiFe ₂ O ₄ /rGO	hydrothermal	1,134.28 F·g ⁻¹	1 A·g⁻¹	19.29 Wh·kg ⁻¹	0.61 kW·kg ⁻¹	76.46% after 5,000 cycles		[219]
Ni0.5Co0.5Fe ₂ O ₄		1,286 F·g ⁻¹	0.5 A·g ⁻¹					[220]
NiFe-A@GNS		845 F·g ⁻¹	1 A·g ⁻¹	30.8 Wh·kg ^{−1}	620 W·kg ^{−1}			[221]
CoF-rGO		551 F·g ⁻¹				98% after 2,000 cycles	2 mV·s ⁻¹	[222]
rGO/MnO ₂ -rod/CuO-		658.97 F·g ⁻¹	1 A·g ⁻¹	118.61 Wh·kg ⁻¹	1.5 kW·kg⁻¹	83.74% after 5,000 cycles		[223]
sphere							\ : :	:
PANI/NiFe ₂ O ₄	in situ oxidative polymerization		1		1	97% after 10,000 cycles	10 mV·s ⁻ '	[224]
Ni/NiFe ₂ O ₄ @C		1,710 C·g¯¹	2 A·g ⁻ '	22 Wh·kg¯'	8,000 W·kg ⁻			[225]
NiFe ₂ O ₄ /rGO		207 F·g	7	Ī	7			[526]
NiTe ₂ -Co ₂ Te ₂ @rGO		223.6 mA·h ⁻ ' g ⁻ '	1 A·g_	51 Wh·kg ⁻¹	800 W·kg ⁻	89.3% after 3,000 cycles		[227]

Table 2: Continued

Material	Synthesis process	Specific capacitance	Current density	Energy density Power density Stability	Power density	Stability	Scan rate References	References
NF/NiFe ₂ O ₄ /carbon NiFe ₂ O ₄ NiFe ₂ O ₄ NiFe2O4	hydrothermal	398 C·g ⁻¹ 240.9 F·g ⁻¹ 541 F·g ⁻¹ 833 F·g ⁻¹	1 A·g ⁻¹ 1 A·g ⁻¹	27.71 Wh·kg ⁻¹ 42 Wh·kg ⁻¹	14.49 kW·kg ⁻¹ 154 W·kg ⁻¹	98% 6,500 cycles 128% after 2,000 cycles 3,000 cycles	2 mV·s ⁻¹	[228] [229] [230] [231]
NiFe ₂ O ₄ and AC NiFe ₂ O ₄	hydrothermal	135 F·g ⁻¹ 240.9 F·g ⁻¹ 262 46 F·g ⁻¹	1 A·g ⁻¹	34.7 Wh·kg ⁻¹ 10.15 Wh·kg ⁻¹	5,314 Wkg ⁻¹ 140 W·kg ⁻¹	88% after 10,000 cycles 128% after 2,000 cycles		[232] [233]
rGO/NIFe ₂ O ₄ rGO/NIFe ₂ O ₄ NiO/NIFe ₂ O ₄ NIFe ₂ O ₄ -rGO	nyarothermai	502.40 F'g 584.63 F:g ⁻¹ 599.9 F:g ⁻¹ 488 F:g ⁻¹	0.05 A'G 1 A·g ⁻¹	56.57 WRPKg 62.5 Wh-kg ⁻¹	2/0.22 KW·kg	2,000 cycles 91% after 2,000 after cycles 86.5% after 2,000 cycles 93.2% after 6,000 cycles		[234] [235] [239]
Zn Fe ₂ O ₄ /NiMoO ₄ rGO/Me Fe ₂ O ₄ rGO/Cu rGO/Mn		147 F.g ⁻¹ 142 F.g ⁻¹ 216 F.g ⁻¹		58.6 Wh·kg ⁻¹	799 W·kg ⁻ '	89.6% after 7,000 cycles 127% up to 100,000 cycles 127% up to 100,000 cycles	5 mV·s ⁻¹	[240] [241] [242] [243]
MnFe ₂ O ₄ /PEDOT/rGO Cobalt ferrite/rGO	hydrothermal one-pot solvothermal technique	298.97 F.g ⁻¹ 551 F.g ⁻¹	1 A·g ⁻¹			81% after 5,000 cycles 8% after 2,000 cycles	2 mV·s ⁻¹ 2 mV·s ⁻¹	[244] [201]
NiFe-A/GNS Ni Fe ₂ O ₄ /NF	chemical vapour deposition hydrothermal	845 F·g ⁻¹ 975 F·g ⁻¹	1–10 A·g ^{–1}	30.8 Wh·kg ⁻¹	620 W·kg ⁻¹	94.3% after 5,000 cycles		[180] [189]

- an issue that requires enhancements in electrode design and material selection [180,235,236].
- c. Cost and scalability: Practical challenges arise from the cost-effectiveness and scalability of supercapacitor technology, particularly in the context of the large-scale synthesis of high-performance electrode materials such as rGO and metal oxides [253-255]. In order to achieve widespread adoption across a variety of sectors, it is imperative to address these challenges [256-258].

Hence, the synthesis processes and synergistic benefits of BMO-rGO composites are discussed, with an emphasis on their superior performance in specific capacitance and cycle stability compared to individual components in comparison with prior studies [259–261]. Thus, this research highlights the potential of BMO-rGO composites as high-performance electrode materials for supercapacitors [262,263]. In addition, the study has exhibited that these composites have showcased their enhanced specific capacitance, improved charge storage capacity, increased power density, excellent cycling stability, and overall durability even after numerous charge-discharge cycles [264,265].

4 Conclusion

We have methodically described both new advancements and traditional approaches pertaining to BMOs as supercapacitor energy storage materials in this study. It is well known that specific surface area and conductivity are two important variables that impact supercapacitor performance when evaluating electrode materials. Graphene, BMOs, and composite materials that mix carbon-based elements with BMOs or other substances are among the materials included in this study. Each material has unique benefits and concerns that make it appropriate for particular supercapacitor kinds and performance needs. Due to its remarkable mechanical and electrical conductivity, graphene has attracted much interest in supercapacitor research. When energy density is high, BMOs like MnO₂ may be considered, although AC is still a dependable option for EDLCs. By integrating the benefits of several materials, composite materials provide a versatile solution. The synergistic effects of composite materials, which combine carbon-based components with BMOs or other compounds, enhance ion/electron diffusion and overall electrochemical performance.

Apart from designating certain structural BMOs, many approaches are used to create composite electrodes. As a result of BMOs' p-type semiconductors, which have a significantly low electric conductivity that makes it difficult for them to support the fast electron transport needed for high rates, mesoporous carbons, graphene, and CNTs combined can be a helpful method for creating rGO-BMObased composite electrodes. The composite material utilizes the advantages of both the conductive EDLC of the carbonaceous material and the pseudocapacitive nature of the metal oxide, suggesting a highly efficient use case for supercapacitors. Additional research has also been used to create rGO-BMO materials with a high specific area. Additional TMO doping may improve performance and create impurity band effects. While significant advancements have been achieved in supercapacitor energy storage for BMOs, there are still issues and roadblocks that need to be resolved in the near future.

Synthetically, it is still quite challenging to create BMOs using a straightforward process that meets all the needs of certain applications. The authors contend that in order to fully realize the promise of BMO-based electrode materials, scientists must optimize the material's characteristics as well as the production settings. Furthermore, achieving extended cycle stability and high specific capacitance still presents a barrier to enhancing rGO-BMO electrochemical performance. Nonetheless, we are excited to support further advancements in this fascinating field of study in order to make significant strides toward supercapacitor applications in the future.

With special benefits including quick charge-discharge cycles, high power density, and a longer lifespan than conventional batteries, supercapacitors, also known as electrochemical capacitors, hold enormous promise as energy storage and conversion devices.

5 Future outlook

- i. Advanced electrode materials: The potential for enhancing energy density, cycle stability, and overall performance is present in the ongoing research of novel electrode materials, including rGO-metal oxide composites like rGO-MnO₂, rGO-Co₃O₄, and rGO-TiO₂. Synergistic effects are provided by these materials, which combine the pseudocapacitive properties of metal oxides with the conductivity of rGO.
- ii. Tailored electrode architectures: The electrochemical performance of supercapacitors can be enhanced further by designing tailored electrode architectures, such as hierarchical composites and 3D nanostructures. These architectural designs provide higher surface area, reduced ion diffusion pathways, and enhanced charge transport, resulting in enhanced cycling stability and raised capacitance.

- iii. Integration with renewable energy systems: The implementation of supercapacitors in conjunction with renewable energy systems, including solar and wind power, offers a promising opportunity to mitigate carbon emissions. Their capacity to store and deliver energy efficiently and their rapid response times complement the intermittent character of renewable energy sources, thereby facilitating easier grid operation and reducing dependence on fossil fuels.
- iv. Continuous improvements in manufacturing methods: the continued development of manufacturing techniques, such as scalable synthesis methods for rGO and metal oxide-based materials, can reduce production costs and enable the widespread deployment of supercapacitor technology. The integration of roll-to-roll processing methods and additive manufacturing offers specifically potential for enhancing scalability as well as cost-effectiveness.

Acknowledgements: The authors extend their appreciation to the Deanship of Scientific Research at King Khalid University (KKU) through the Research Group Program Under the Grant Number: (R.G.P.2/382/44).

Funding information: The authors extend their appreciation to the Deanship of Scientific Research at King Khalid University (KKU) through the Research Group Program Under the Grant Number: (R.G.P.2/382/44).

Author contributions: Conceptualization, KK, AJ, RK, SS, PSB, AS; formal analysis, KK, AJ, RK, SS, PSB, AS; investigation, KK, AJ, RK, SS, PSB, AS; writing – original draft preparation, KK, AJ, RK, SS, PSB, AS; writing – review and editing, SS, AS, SKJ, DK, MA, JL; supervision, SS, AS, SKJ, DK, MA, JL; project administration, SS, AS, SKJ, DK, MA, JL; funding acquisition, SS, SKJ, DK, MA, JL. All authors have read and agreed to the published version of the manuscript.

Conflict of interest: Authors state no conflict of interest.

Data availability statement: The datasets generated during and/or analyzed during the current study are available from the corresponding author on reasonable request.

References

[1] Zhang Z, Ding T, Zhou Q, Sun Y, Qu M, Zeng Z, et al. A review of technologies and applications on versatile energy storage systems. Renew Sustain Energy Rev. (2021);148:111263.

- [2] Varun RP, Bhat IK. Energy, economics and environmental impacts of renewable energy systems. Renew Sustain Energy Rev. 2009;13:2716–21. doi: 10.1016/j.rser.2009.05.007.
- [3] Panwar NL, Kaushik SC, Kothari S. Role of renewable energy sources in environmental protection: a review. Renew Sustain Energy Rev. 2011;15:1513–24. doi: 10.1016/j.rser.2010.11.037.
- [4] Simon P, Gogotsi Y. Materials for electrochemical capacitors. Nat Mater. 2008;7:845–54. doi: 10.1142/9789814287005 0033.
- [5] Dunn B, Kamath H, Tarascon JM. Electrical energy storage for the grid: a battery of choices. Science. 2011;334:927–35. doi: 10.1126/ science. 1212741.
- [6] Miller JR, Burke AF. Electrochemical capacitors: challenges and opportunities for real-world applications. Electrochem Soc Interface. 2008:17:53–7.
- [7] Crabtree G. The energy-storage revolution. Nature. 2015;526:S92.
- [8] Shabangoli Y, Rahmanifar MS, El-Kady MF, Noori A, Mousavi MF, Kaner RB. An integrated electrochemical device based on earth-abundant metals for both energy storage and conversion. Energy Storage Mater. 2018;11:282–93. doi: 10.1016/j.ensm.2017. 09.010.
- [9] Ellabban O, Abu-Rub H, Blaabjerg F. Renewable energy resources: current status, future prospects and their enabling technology. Renew Sustain Energy Rev. 2014;39:748–64. doi: 10.1016/j.rser. 2014.07.113.
- [10] El-Kady MF, Shao Y, Kaner RB. Graphene for batteries, supercapacitors and beyond. Nat Rev Mater. 2016;1:16033. doi: 10.1038/ natrevmats.2016.33.
- [11] El-Kady MF, Ihns M, Li M, Hwang JY, Mousavi MF, Chaney L, et al. Engineering three-dimensional hybrid supercapacitors and microsupercapacitors for high-performance integrated energy storage. Proc Natl Acad Sci U S A. 2015;112:4233–8. doi: 10.1073/pnas.1420398112.
- [12] Yu Z, Tetard L, Zhai L, Thomas J. Supercapacitor electrode materials: Nanostructures from 0 to 3 dimensions. Energy Environ Sci. 2015;8:702–30. doi: 10.1039/c4ee03229b.
- [13] Wang Y, Song Y, Xia Y. Electrochemical capacitors: mechanism, materials, systems, characterization and applications. Chem Soc Rev. 2016;45:5925–50. doi: 10.1039/c5cs00580a.
- [14] Choudhary N, Li C, Moore J, Nagaiah N, Zhai L, Jung Y, et al. Asymmetric supercapacitor electrodes and devices. Adv Mater. 2017;29(21):1605336. doi: 10.1002/adma.201605336.
- [15] Huang Y, Li H, Wang Z, Zhu M, Pei Z, Xue Q, et al. Nanostructured Polypyrrole as a flexible electrode material of supercapacitor. Nano Energy. 2016;22:422–38. doi: 10.1016/j.nanoen.2016.02.047.
- Simon P, Gogotsi Y, Dunn B. Where do batteries end and supercapacitors begin? Science. 2014;343:1210–1. doi: 10.1126/science. 1249625.
- [17] Pandolfo AG, Hollenkamp AF. Carbon properties and their role in supercapacitors. J Power Sources. 2006;157:11–27. doi: 10.1016/j. jpowsour.2006.02.065.
- [18] Yassine M, Fabris D. Performance of commercially available supercapacitors. Energies. 2017;10:1340. doi: 10.3390/ en10091340.
- [19] Yu A, Chabot V, Zhang J. Electrochemical supercapacitors for energy storage and delivery- fundamental and application. Boca Raton: CRC Press, Taylor & Francis Group.
- [20] Saikia BK, Benoy SM, Bora M, Tamuly J, Pandey M, Bhattacharya D. A brief review on supercapacitor energy storage devices and utilization of natural carbon resources as their electrode materials. Fuel. 2020;282:118796.

- [21] Iro ZS, Subramani C, Dash SS. A brief review on electrode materials for supercapacitor. Int J Electrochem Sci. 2016;11:10628–43. doi: 10.20964/2016.12.50.
- [22] Ho J, Jow TR, Boggs S. Historical introduction to capacitor technology. IEEE Electr Insul Mag. 2010;26(1):20–5. doi: 10.1109/mei. 2010.5383924.
- [23] Olabi AG, Abdelkareem MA, Wilberforce T, Sayed ET. Application of graphene in energy storage device – A review. Renew Sustain Energy Rev. 2021;135:110026.
- [24] Baroutaji A, Wilberforce T, Ramadan M, Olabi AG. Comprehensive investigation on hydrogen and fuel cell technology in the aviation and aerospace sectors. Renew Sustain Energy Rev. 2019;106:31–40. doi: 10.1016/j.rser.2019.02.022.
- [25] Wilberforce T, Hassan ZE, Durrant A, Thompson J, Soudan B, Olabi AG. Overview of ocean power technology. Energy. 2019;175:165–81. doi: 10.1016/j.energy.2019.03.068.
- [26] Wilberforce T, Baroutaji A, Hassan ZE, Thompson J, Soudan B, Olabi AG. Prospects and challenges of concentrated solar photovoltaics and enhanced geothermal energy technologies. Sci Total Environ. April 2019;659:851–61. doi: 10.1016/j.scitotenv.2018. 12.257.
- [27] Wilberforce T, Baroutaji A, Soudan B, Al-Alami AH, Olabi AG. Outlook of carbon capture technology and challenges. Sci Total Environ. 20 March 2019;657:56–72. doi: 10.1016/j.scitotenv.2018. 11 424.
- [28] Wilberforce T, Olabi AG. Design of experiment (DOE) analysis of 5-cell stack fuel cell using three bipolar plate geometry design. Sustainability. 2020;12:4488. doi: 10.3390/su12114488.
- [29] Wilberforce T, Olabi AG. Performance prediction of proton exchange membrane fuel cells (PEMFC) using adaptive neuro inference system (ANFIS). Sustainability. 2020;12:4952. doi: 10. 3390/su12124952
- [30] Ogungbemi E, Ijaodola O, Khatib FN, Wilberforce T, El Hassan Z, Thompson J, et al. Fuel cell membranes – pros and cons. Energy. 2019;172:155–72. doi: 10.1016/J.ENERGY.2019.01.034.
- [31] Chen T, Dai L. Carbon nanomaterials for high performance supercapacitors. Mater Today. 2013;16(7/8):272–80. doi: 10. 1016/ i.mattod.2013.07.002.
- [32] Xia JL, Chen F, Li JH, Tao NJ. Measurement of the quantum capacitance of graphene. Nat Nanotechnol. 2009;4:505–9. doi: 10. 1038/nnano.2009.177.
- [33] Meng Q, Cai K, Chen Y, Chen L. Research progress on conducting polymer based supercapacitor electrode materials. Nano Energy. 2017;36:268–85. doi: 10.1016/j.nanoen.2017.04.040.
- [34] Wang G, Zhang L, Zhang J. A review of electrode materials for electrochemical supercapacitors. Chem Soc Rev. 2012;41:797–828. doi: 10.1039/1cs15060j.
- [35] Vangari M, Pryor T, Jiang L. Supercapacitors: review of materials and fabrication methods. J Energy Eng. 2013;139(2):72–9. doi: 10. 1061/(ASCE)EY.1943-7897.0000102.
- [36] Zhang LL, Zhao XS. Carbon-based materials as supercapacitor electrodes. Chem Soc Rev. 2009;38:2520.
- [37] Lu M, Benguin F, Frackowiak E. Supercapacitors: Materials, systems, and applications. Weinheim, Germany: Wiley-VCH; 2013. p. 207.
- [38] Burke A. Ultracapacitors: Why, how, and where is the technology. J Power Sources. 2000;91:37.
- [39] Hall PJ, Bain EJ. Energy-storage technologies and electricity generation. Energy Policy. 2008;36:4352.

- [40] Hadjipaschalis I, Poullikkas A, Efthimiou V. Overview of current and future energy storage technologies for electric power applications. Renew Sustain Energy Rev. 2009;13:1513.
- [41] John H. In NASA-Tech Briefs: Engineering Solutions for Design & Manufacturing. Cleveland, OH, USA: Glenn Research Center; 2007.
- [42] Smith TA, Mars JP, Turner GA. 2002 IEEE 33rd Annual Power Electronics Specialists Conf., PESC 02. 1, Piscataway, NJ, USA: IEEE; 2002. p. 124. doi: 10.1109/PSEC.2002.1023857.
- [43] German J. Hybrid vehicles: Technology development and cost reduction. ICCT Technical Brief No. 1; July 2015.
- [44] Maxwell Technologies, Inc.. http://www.maxwell.com/solutions/ transportation/auto/start-stop-micro-hybrid (accessed: Feb 07, 2017).
- [45] Naswali E, Alexander C, Han HY, Naviaux D, Bistrika A, Jouanne AV, et al. 2011 IEEE Energy Conversion Congress, Exposition. Piscataway, NJ, USA: IEEE; 2011. p. 298. doi: 10.1109/ECCE.2011. 6063783.
- [46] Wang X, Lu X, Liu B, Chen D, Tong Y, Shen G. Flexible energystorage devices: design consideration and recent progress. Adv Mater. 2014;26:4763.
- [47] Li L, Wu Z, Yuan S, Zhang X-B. Advances and challenges for flexible energy storage and conversion devices and systems. Energy Env. Sci. 2014;7:2101.
- [48] Mirvakili SM, Mirvakili MN, Englezos P, Madden JDW, Hunter IW. High Performance Supercapacitors from Niobium Nanowire Yarns. ACS Appl Mater Interfaces. 2015;7:13882.
- [49] Lu X, Yu M, Wang G, Tong Y, Li Y. Flexible solid-state supercapacitors: design, fabrication and applications. Energy Env. Sci. 2014;7:2160.
- [50] Lu X, Li G, Tong Y. A review of negative electrode materials for electrochemical supercapacitors. Sci China. Ser E: Technol Sci. 2015;58:1799
- [51] Vangari M, Pryor T, Jiang L. Supercapacitors: Review of materials and fabrication methods. J Energy Eng. 2013;139:72.
- [52] Xia H, Hong C, Li B, Zhao B, Lin Z, Zheng M, et al. Facile synthesis of hematite quantum-dot/functionalized graphene-sheet composites as advanced anode materials for asymmetric supercapacitors. Adv Funct Mater. 2015;25:627.
- [53] Wu ZS, Ren W, Wang DW, Li F, Liu B, Cheng HM. High-energy MnO₂ nanowire/graphene and graphene asymmetric electrochemical capacitors. ACS Nano. 2010 Oct 26;4(10):5835–42. doi: 10.1021/nn101754k. PMID: 20857919.
- [54] Zhu Y, Murali S, Cai W, Li X, Suk JW, Potts JR, et al. Graphene and graphene oxide: synthesis, properties, and applications. Adv Mater. 2010;22:3906.
- [55] Simon P, Gogotsi Y. Materials for electrochemical capacitors. Nat Mater. 2008;7:845.
- [56] Xie K, Wei B. Materials and structures for stretchable energy storage and conversion devices. Adv Mater. 2014;26:3592.
- [57] Bo Z, Shuai X, Mao S, Yang H, Qian J, Chen J, et al. Green preparation of reduced graphene oxide for sensing and energy storage applications. Sci Rep. 2014;4:1–8.
- [58] Geim AK, Novoselov KS. The rise of graphene. Nat Mater. 2007;6:183.
- [59] Singh V, Joung D, Zhai L, Das S. Graphene based materials: Past, present and future. Prog Mater Sci. 2011;56:1178.
- [60] Informa F, Number WR, House M, Street M, Schafhaeutl C, Version M. Through silicon vias: materials, models, design, and performance. Philos Mag Ser. 2009;3:570.

- Brodie BC. On the atomic weight of graphite. Philos Trans R Scoc Lond. 1859:149:249.
- [62] Zhao X, Zhang Q, Hao Y, Li Y, Fang Y, Chen D. Alternate multilayer films of poly(vinyl alcohol) and exfoliated graphene oxide fabricated via a facial layer-by-layer assembly. Macromolecules. 2010;43:9411.
- Schniepp HC, Li JL, McAllister MJ, Sai H, Herrera-Alonson M, [63] Adamson DH, et al. Functionalized single graphene sheets derived from splitting graphite oxide. J Phys Chem B. 2006;110:8535.
- [64] Pei S, Cheng HM. The reduction of graphene oxide. Carbon NY. 2012;50:3210.
- Hirata M, Gotou T, Ohba M. Thin-film particles of graphite oxide. 2: Preliminary studies for internal micro fabrication of single particle and carbonaceous electronic circuits. Carbon NY. 2005:43:503.
- Hummers Jr WS, Offeman RE. Preparation of graphitic oxide. J Am [66] Chem Soc. 1958;80:1339.
- [67] Brodie B. On the atomic weight of graphite. Proc R Soc Lond. 1859;10:11-2.
- [68] Staudenmaier L. Method for representing the graphite acid. Ber Dtsch Chem Ges. 1898;31:1481-7.
- Stankovich S, Dikin DA, Piner RD, Kohlhaas KA, Kleinhammes A, [69] Jia Y, et al. Synthesis of graphene-based nanosheets via chemical reduction of exfoliated graphite oxide. Carbon. 2007;45:1558-65.
- [70] Shin HJ, Kim KK, Benayad A, Yoon SM, Park HK, Jung IS, et al. Efficient reduction of graphite oxide by sodium borohydride and its effect on electrical conductance. Adv Funct Mater. 2009;19:1987-92.
- [71] Parades JI, Villar-Rodil S, Martínez-Alonso A, Tascón JMD. Graphene oxide dispersions in organic solvents. Langmuir. 2008;24(19):10560-4.
- [72] Lu J, Drzal LT, Worden RM, Lee I. Simple fabrication of a highly sensitive glucose biosensor using enzymes immobilized in exfoliated graphite nanoplatelets nafion membrane. Chem Mater. 2007;19(25):6240-6.
- [73] Mao S, Pu H, Chen J. Graphene oxide and its reduction: modeling and experimental progress. RSC Adv. 2012;2:2643-62.
- [74] Hong Y, Wang Z, Jin X. Sulfuric acid intercalated graphite oxide for graphene preparation. Sci Rep. 2013;3:3439.
- Wan W, Zhao Z, Hu H, Gogotsi Y, Qiu J. Highly controllable and [75] green reduction of graphene oxide to flexible graphene film with high strength. Mater Res Bull. 2013;48:4797-803.
- [76] Berger C, Song Z, Li X, Wu X, Brown N, Naud C, et al. Electronic confinement and coherence in patterned epitaxial graphene. Science. 2006;312:1191-6.
- [77] Bo Z, Yu K, Lu G, Wang P, Mao S, Chen J. Understanding growth of carbon nanowalls at atmospheric pressure using normal glow discharge plasma-enhanced chemical vapor deposition. Carbon. 2011;49:1849-58.
- [78] Hernandez Y, Nicolosi V, Lotya M, Blighe FM, Sun Z, De S, et al. High-yield production of graphene by liquid-phase exfoliation of graphite. Nat Nanotechnol. 2008;3:563-8.
- [79] Sutter PW, Flege JI, Sutter EA. Epitaxial graphene on ruthenium. Nat Mater. 2008;7:406-11.
- Sun Z, Yan Z, Yao J, Beitler E, Zhu Y, Tour JM. Growth of graphene from solid carbon sources. Nature. 2010;468:549-52.
- [81] Malik S, Vijayaraghavan A, Erni R, Ariga K, Khalakhan I, Hill JP. High purity graphenes prepared by a chemical intercalation method. Nanoscale. 2010;2:2139-43. Mater Sci.

- Zhu AY, Cubukcu E. Graphene nanophotonic sensors. 2D Mater. 2015:2:032005-15.
- [83] Leng K, Zhang F, Zhang L, Zhang T, Wu Y, Lu Y, et al. Graphenebased Li-ion hybrid supercapacitors with ultrahigh performance. Nano Res. 2013;6:581-92.
- [84] Spyrou K, Gournis D, Rudolf P. Hydrogen storage in graphenebased materials: efforts towards enhanced hydrogen absorption. ECS I Solid State Sci Technol. 2013;2:M3160-9.
- [85] Huang X, Qi X, Boey F, Zhang H. Graphene-based composites. Chem Soc Rev. 2012;41:666-86.
- Li N, Zheng M, Lu H, Hu Z, Shen C, Chang X, et al. High-rate [86] lithium-sulfur batteries promoted by reduced graphene oxide coating. Chem Commun. 2012;48:4106-8.
- [87] Torrisi F. Hasan T. Wu W. Sun Z. Lombardo A. Kulmala T. et al. Inkjet-printed graphene electronics. ACS Nano. 2012;6:2992-3006.
- [88] Park H, Brown P, Bulovi V, Kong J. Graphene as transparent conducting electrodes in organic photovoltaics: studies in graphene morphology, hole transporting layers, and counter electrodes. Nano Lett. 2012;12:133-40.
- [89] Kim SB, Park JY, Kim CS, Okuyama K, Lee SE, Jang HD, et al. Effects of graphene in dye-sensitized solar cells based on nitrogen-doped TiO2 composite. J Phys Chem C. 2015;119:16552-9.
- [90] Kashyout AB, Soliman M, Fathy M. Effect of preparation parameters on the properties of TiO2 nanoparticles for dye sensitized solar cells. Renewable Energy. 2010;35:2914-20.
- [91] Liu J, Cui L, Losic D. Graphene and graphene oxide as new nanocarriers for drug delivery applications. Acta Biomater. 2013;9:9243-57.
- [92] Yang Y, Asiri AM, Tang Z, Du D, Lin Y. Graphene based materials for biomedical applications. Mater Today. 2013;16:365-73.
- Obodo RM, Nwanya AC, Iroegbu C, Ahmad I, Ekwealor AB, Osuji R, et al. Transformation of GO to rGO due to 8.0 MeV carbon (C++) ions irradiation and characteristics performance on MnO2-NiO-ZnO@ GO electrode. Int | Energy Res. 2020;44(8):6792-803.
- [94] Zeyrek Ongun M, Oguzlar S, Doluel EC, Kartal U, Yurddaskal M. Enhancement of piezoelectric energy-harvesting capacity of electrospun β-PVDF nanogenerators by adding GO and rGO. I Mater Sci: Mater Electron. 2020:31:1960-8.
- [95] Jindal H, Oberoi AS, Sandhu IS, Chitkara M, Singh B. Graphene for hydrogen energy storage-a comparative study on GO and rGO employed in a modified reversible PEM fuel cell. Int J Energy Res. 2021;45(4):5815-26.
- Malik MTU, Sarker A, Rahat SSM, Shuchi SB. Performance [96] enhancement of graphene/GO/rGO based supercapacitors: A comparative review. Mater Today Commun. 2021;28:102685.
- [97] Ikram M, Raza A, Imran M, Ul-Hamid A, Shahbaz A, Ali S. Hydrothermal synthesis of silver decorated reduced graphene oxide (rGO) nanoflakes with effective photocatalytic activity for wastewater treatment. Nanoscale Res Lett. 2020;15:1-11.
- [98] Brisebois PP, Siaj M. Harvesting graphene oxide-years 1859 to 2019: a review of its structure, synthesis, properties and exfoliation. J Mater Chem C. 2020;8(5):1517-47.
- [99] Staudenmaier L. Verfahren zur darstellung der graphitsäure. Ber Dtsch Chem Ges. 1898;31:1481.
- [100] Hofmann U, Konig E. Studies on graphite oxide. J Anorg Allg Chem. 1937;234(4):311-36.
- [101] Hofmann U, Hoist R. About the acidification and methylation of graphite oxide. Ber Dtsch Chem Ges. 1939;72(4):754-71.

- Hummers WS, Offeman RE. Preparation of graphitic oxide. J Am Chem Soc. 1958;80:1339.
- [103] McAllister MJ, Li J, Adamson DH, Schniepp HC, Abdala AA, Liu J, et al. Single sheet functionalized graphene by oxidation and thermal expansion of graphite. Chem Mater. 2007;19:4396.
- [104] David L, Bhandavat R, Singh G. MoS2/graphene composite paper for sodium-ion battery electrodes. ACS Nano. 2014;8(2):1-13.
- [105] Surekha G, Krishnaiah KV, Ravi N, Suvarna RP. FTIR, Raman and XRD analysis of graphene oxide films prepared by modified Hummers method. J Physics: Conf Ser. 2020, March;1495(1):012012. IOP Publishing.
- [106] Santamaría-Juárez G, Gómez-Barojas E, Quiroga-González E, Sánchez-Mora E, Quintana-Ruiz M, Santamaría-Juárez JD. Safer modified Hummers' method for the synthesis of graphene oxide with high quality and high yield. Mater Res Express. 2020;6(12):125631.
- [107] Riahi KZ, Sdiri N, Ennigrou DJ, Horchani-Naifer K. Investigations on electrical conductivity and dielectric properties of graphene oxide nanosheets synthetized from modified Hummer's method. J Mol Structure. 2020;1216:128304.
- [108] Costa MC, Marangoni VS, Ng PR, Nguyen HT, Carvalho A, Castro Neto AH. Accelerated synthesis of graphene oxide from graphene. Nanomaterials. 2021;11(2):551.
- [109] Gaidukevic J, Aukstakojyte R, Navickas T, Pauliukaite R, Barkauskas J. A novel approach to prepare highly oxidized graphene oxide: Structural and electrochemical investigations. Appl Surf Sci. 2021;567:150883.
- [110] Habte AT, Ayele DW. Synthesis and characterization of reduced graphene oxide (rGO) started from graphene oxide (GO) using the tour method with different parameters. Adv Mater Sci Eng. 2019;2019:1-9.
- Alam SN, Sharma N, Kumar L. Synthesis of graphene oxide (GO) by modified hummers method and its thermal reduction to obtain reduced graphene oxide (rGO). Graphene. 2017;6(1):1-18.
- [112] Zhu J, Zu J, Liu J, Wang Y, Pei M, Xu Y. Self-assembled reduced graphene oxide films with different thicknesses as high performance supercapacitor electrodes. J Energy Storage. 2020:32:101795.
- [113] Marcelina V, Syakir N, Wyantuti S, Hartati YW, Hidayat R. Characteristic of thermally reduced graphene oxide as supercapacitors electrode materials. In IOP Conference Series: Materials Science and Engineering. Vol. 196, Issue 1, IOP Publishing; 2017, May. p. 012034.
- [114] Rasul S, Alazmi A, Jaouen K, Hedhili MN, Costa PMFJ. Rational design of reduced graphene oxide for superior performance of supercapacitor electrodes. Carbon. 2017;111:774-81.
- Saha U, Jaiswal R, Goswami TH. A facile bulk production of processable partially reduced graphene oxide as superior supercapacitor electrode material. Electrochim Acta. 2016;196:386-404.
- Mathew DS, Juang RS. An overview of the structure and magnetism of spinel ferrite nanoparticles and their synthesis in microemulsions. Chem Eng J. 2007;129:51-65.
- Yadav RS, Havlica J, Masilko J, Kalina L, Wasserbauer J, [117] Hajdúchová M, et al. Impact of Nd³⁺ in CoFe₂O₄ spinel ferrite nanoparticles on cation distribution, structural and magnetic properties. J Magn Magn Mater. 2016;399:109-17.
- Marinca TF, Chicinas I, Isnard O. Structural and magnetic properties of the copper ferrite obtained by reactive milling and heat treatment. Ceram Int. 2013;39:4179-86.

- [119] Cullity BD, Graham CD. Introduction to magnetic materials. Mater Today. 2009;12:45.
- [120] Kuanr BK, Mishra SR, Wang L, Delconte D, Neupane D, Veerakumar V, et al. Frequency and field dependent dynamic properties of CoFe₂-xAlxO₄ ferrite nanoparticles. Mater Res Bull. 2016:76:22-7.
- Anik MI, Khalid Hossain M, Hossain I, Mahfuz AMUB, Tayebur Rahman M, Ahmed I. Recent progress of magnetic nanoparticles in biomedical applications: A review. Nano Select. 2021;2(6):1146-86.
- [122] Mahmoud ME, Abdelwahab MS, Fathallah EM. Design of novel nano-sorbents based on nano-magnetic iron oxide-bound-nanosilicon oxide-immobilized-triethylenetetramine for implementation in water treatment of heavy metals. Chem Eng J. 2013;223:318-27.
- [123] Meng Q, Wang Z, Chai X, Weng Z, Ding R, Dong L. Fabrication of hematite (α-Fe2O3) nanoparticles using electrochemical deposition. Appl Surf Sci. 2016;368:303-8.
- [124] Narang SB, Pubby K. Nickel spinel ferrites: a review. J Magnetism Magnetic Mater. 2021;519:167163.
- Khoso WA, Haleem N, Baig MA, Jamal Y. Synthesis, characteriza-[125] tion and heavy metal removal efficiency of nickel ferrite nanoparticles (NFN's). Sci Rep. 2021;11(1):3790.
- [126] Senthilkumar N, Vivek E, Shankar M, Meena M, Vimalan M, Vetha Potheher I. Synthesis of ZnO nanorods by one step microwaveassisted hydrothermal route for electronic device applications. J Mater Sci: Mater Electron. 2018;29:2927-38.
- Bokov D, Turki Jalil A, Chupradit S, Suksatan W, Javed Ansari M, [127] Shewael IH, et al. Nanomaterial by sol-gel method: synthesis and application. Adv Mater Sci Eng. 2021;2021(1):5102014.
- [128] Rana G, Dhiman P, Kumar A, Vo DVN, Sharma G, Sharma S, et al. Recent advances on nickel nano-ferrite: A review on processing techniques, properties and diverse applications. Chem Eng Res Des. 2021:175:182-208.
- [129] Li J, Feng H, Jiang J, Feng Y, Xu Z, Dong Q. One-pot in situ synthesis of a CoFe2O4 nanoparticle-reduced graphene oxide nanocomposite with high performance for levodopa sensing. RSC Adv.
- Burianova S, Vejpravova JP, Holec P, Plocek J, Niznansky D. Surface [130] spin effects in La-doped CoFe2O4 nanoparticles prepared by microemulsion route. J Appl Phys. 2011;110:073902.
- Nivetha R, Santhosh C, Kollu P, Jeong S-K, Bhatnagar A, Grace AN. [131] Cobalt and nickel ferrites based graphene nanocomposites for electrochemical hydrogen evolution. J Magn Magn Mater. 2018;448:165-71.
- [132] Zhang X, Sun J, Chen T, Xiang C, Zhao Y, Zhang N. Hydrothermal synthesis of Pd-doped rGO/ZnO-SnO2 nanocomposites for efficient hydrogen detection. Ionics. 2022;28(6):3013-21.
- [133] Liu P, Chen H, Chang X, Xue Y, Zhou J, Zhao Z, et al. Novel method of preparing CoFe2O4/graphene by using steel rolling sludge for supercapacitor. Electrochim Acta. 2017;231:565-74.
- [134] Govindasamy M, Wang S-F, Kumaravel S, Ramalingam RJ, Allohedan HA. Facile synthesis of copper sulfide decorated reduced graphene oxide nanocomposite for high sensitive detection of toxic antibiotic in milk. Ultrason Sonochem. 2018;56:193-9.
- Carmel Jeeva Mary B, Judith Vijaya J, Bououdina M, John Kennedy L, Khezami L, Modwi A. Adsorption ability of aqueous lead (II) by NiFe2O4 and 2D-rGO decorated NiFe2O4 nanocomposite. J Mater Sci: Mater Electron. 2023;34(9):845.

- [136] Sousa MH, Tourinho FA, Depeyrot J, da Silva GJ, Lara MCF. New electric double-layered magnetic fluids based on copper, nickel, and zinc ferrite nanostructures. J Phys Chem B. 2001;105:1168–75.
- [137] Mani V, Devadas B, Chen S-M. Direct electrochemistry of glucose oxidase at electrochemically reduced graphene oxide-multiwalled carbon nanotubes hybrid material modified electrode for glucose biosensor. Biosens Bioelectron. 2013;41:309–15.
- [138] Mani V, Dinesh B, Chen S-M, Saraswathi R. Direct electrochemistry of myoglobin at reduced graphene oxide-multiwalled carbon nanotubes-platinum nanoparticles nanocomposite and biosensing towards hydrogen peroxide and nitrite. Biosens Bioelectron. 2014;53:420–7.
- [139] Zhu M, Meng D, Wang C, Diao G. Facile fabrication of hierarchically porous CuFe2O4 nanospheres with enhanced capacitance property. ACS Appl Mater Interfaces. 2013;5(13):6030–7.
- [140] Wang J, Deng Q, Li M, Jiang K, Zhang J, Hu Z, et al. Copper ferrites@reduced graphene oxide anode materials for advanced lithium storage applications. Sci Rep. 2017;7(1):8903.
- [141] Fu Y, Chen Q, He M, Wan Y, Sun X, Xia H, et al. Copper ferritegraphene hybrid: A multifunctional heteroarchitecture for photocatalysis and energy storage. Ind & Eng Chem Res. 2016;51(36):11700–9.
- [142] Luo L, Cui R, Qiao H, Chen K, Fei Y, Li D, et al. High lithium electroactivity of electrospun CuFe2O4 nanofibers as anode material for lithium-ion batteries. Electrochim Acta. 2014:144:85–91
- [143] Aparna ML, Grace AN, Sathyanarayanan P, Sahu NK. A comparative study on the supercapacitive behaviour of solvothermally prepared metal ferrite (MFe₂O₄, M = Fe, Co, Ni, Mn, Cu, Zn) nanoassemblies. J Alloy Compd. 2018;745:385–95.
- [144] Gao X, Wang W, Bi J, Chen Y, Hao X, Sun X, et al. Morphologycontrollable preparation of NiFe2O4 as high performance electrode material for supercapacitor. Electrochim Acta. 2019;296:181–9.
- [145] Hazra S, Patra MK, Vadera SR, Ghosh NN. A novel but simple "One-Pot" synthetic route for preparation of (NiFe2O4) x-(BaFe12O19) 1- x composites. J Am Ceram Soc. 2012;95(1):60-3.
- [146] Kooti M, Sedeh AN. Synthesis and characterization of NiFe2O4 magnetic nanoparticles by combustion method. J Mater Sci & Technol. 2013;29(1):34–8.
- [147] Shafi KV, Koltypin Y, Gedanken A, Prozorov R, Balogh J, Lendvai J, et al. Sonochemical preparation of nanosized amorphous NiFe2O4 particles. J Phys Chem B. 1997;101(33):6409–14.
- [148] Sivakumar P, Ramesh R, Ramanand A, Ponnusamy S, Muthamizhchelvan C. Preparation and properties of nickel ferrite (NiFe2O4) nanoparticles via sol-gel auto-combustion method. Mater Res Bull. 2011;46(12):2204–7.
- [149] Kombaiah K, Vijaya JJ, Kennedy LJ, Kaviyarasu K. Catalytic studies of NiFe2O4 nanoparticles prepared by conventional and microwave combustion method. Mater Chem Phys. 2019;221:11–28.
- [150] Sivakumar P, Ramesh R, Ramanand A, Ponnusamy S, Muthamizhchelvan C. Preparation and properties of NiFe2O4 nanowires. Mater Lett. 2012;66(1):314–7.
- [151] Sen R, Jain P, Patidar R, Srivastava S, Rana RS, Gupta N. Synthesis and characterization of nickel ferrite (NiFe2O4) nanoparticles prepared by sol-gel method. Mater Today: Proc. 2015;2(4–5):3750–7.
- [152] Bernaoui CR, Bendraoua A, Zaoui F, Gallardo JJ, Navas J, Boudia RA, et al. Synthesis and characterization of NiFe2O4 nanoparticles as reusable magnetic nanocatalyst for organic dyes

- catalytic reduction: study of the counter anion effect. Mater Chem Phys. 2022;292:126793.
- [153] Taylor AK, Prabhudev S, Botton GA, Gates BD. Assessing the transformations of supported nanocatalysts used in the oxygen evolution reaction: a case study using nife2o4 nanoparticles supported on textured Ni electrodes. ACS Appl Energy Mater. 2022;5(11):13222–33.
- [154] Benlembarek M, Salhi N, Benrabaa R, Boulahouache A, Trari M. Enhanced photocatalytic performance of NiFe2O4 nanoparticle spinel for hydrogen production. Int J Hydrog Energy. 2023;48(24):8932–42.
- [155] Said AA, Abu-Sehly AA, Mahmoud AZ, Ahmed H, Goda MN. Influence of ultrasonic radiation on the structural, magnetic, electrical, and catalytic properties of NiFe2O4 nanoparticles. I Mater Science: Mater Electron. 2022;33(21):16805–17.
- [156] Divya S, Sivaprakash P, Raja S, Muthu SE, Eed EM, Arumugam S, et al. Temperature-dependent dielectric and magnetic properties of NiFe2O4 nanoparticles. Appl Nanosci. 2023;13(2):1327–36.
- [157] Mowlika V, Naveen CS, Phani AR, Sivakumar A, Dhas SMB, Robert R. Crystallographic and magnetic phase stabilities of NiFe2O4 nanoparticles at shocked conditions. J Mater Science: Mater Electron. 2020;31(17):14851–8.
- [158] Bhojane P, Sharma A, Pusty M, Kumar Y, Sen S, Shirage P. Synthesis of ammonia-assisted porous nickel ferrite (NiFe2O4) nanostructures as an electrode material for supercapacitors. I Nanosci Nanotechnol. 2017;17(2):1387–92.
- [159] Patil PD, Shingte SR, Karade VC, Kim JH, Dongale TD, Mujawar SH, et al. Effect of annealing temperature on morphologies of metal organic framework derived NiFe2O4 for supercapacitor application. J Energy Storage. 2021;40:102821.
- [160] Toghan A, Khairy M, Kamar EM, Mousa MA. Effect of particle size and morphological structure on the physical properties of NiFe2O4 for supercapacitor application. J Mater Res Technol. 2022;19:3521–35.
- [161] Wang H, Wang J, Cao D, Gu H, Li B, Lu X, et al. J Mater Chem A. 2017;5:6817–24.
- [162] Xu B, Zhang J, Gu Y, Zhang Z, Al Abdulla W, Kumar NA, et al. Lithium-storage properties of gallic acid-reduced graphene oxide and silicon-graphene composites. Electrochim Acta. 2016;212:473–80.
- [163] Chen W, Li S, Chen C, Yan L. Self-assembly and embedding of nanoparticles by in situ reduced graphene for preparation of a 3D graphene/nanoparticle aerogel. Adv Mater. 2011;23:5679–83.
- [164] Tan Q, Kong X, Guan X, Wang C, Xu B. Crystallization of zinc oxide quantum dots on graphene sheets as an anode material for lithium ion batteries. CrystEngComm. 2020;22:320–9.
- [165] Wang J, Wang H, Li F, Xie S, Xu G, She Y, et al. Oxidizing solid Co into hollow Co₃O₄ within electrospun (carbon) nanofibers towards enhanced lithium storage performance. J Mater Chem A. 2019;7:3024–30.
- [166] Liu D, Kong Z, Liu X, Fu A, Wang Y, Guo Y-G, et al. Spray-drying-induced assembly of Skeleton-structured SnO₂/graphene composite spheres as superior anode materials for high-performance lithium-ion batteries. Mater Interfaces. 2018;10:2515–25.
- [167] Chen M, Zhang C, Li L, Liu Y, Li X, Xu X, et al. Sn powder as reducing agents and SnO₂ precursors for the synthesis of SnO₂reduced graphene oxide hybrid nanoparticles. Mater Interfaces. 2013;5:13333–39.

- Hao J, Ji L, Wu K, Yang N. Electrochemistry of ZnO@reduced graphene oxides. Carbon. 2018;130:480-6.
- [169] Xu B, Guan X, Zhang LY, Liu X, Jiao Z, Liu X, et al. A simple route to preparing y-Fe₂O₃/RGO composite electrode materials for lithium ion batteries. J Mater Chem A. 2018;6:4048-54.
- [170] Xu B, Dai X, Tan Q, Wei Y, Liu G, Wu G. Controlled engineering of nano-sized FeOOH@ZnO hetero-structures on reduced graphene oxide for lithium-ion storage and photo-Fenton reaction. CrystEngComm. 2020;22:2827-36.
- [171] Tan Q, Kong Z, Chen X, Zhang L, Hu X, Mu M, et al. Synthesis of SnO2/graphene composite anode materials for lithium-ion batteries. Appl Surf Sci. 2019;485:314-22.
- Tan Q, Kong Z, Guan X, Zhang LY, Jiao Z, Chen HC, et al. Hierarchical zinc oxide/reduced graphene oxide composite: Preparation route, mechanism study and lithium ion storage. I Colloid Interface Sci. 2019;548:233-43.
- [173] Modafferi V, Santangelo S, Fiore M, Fazio E, Triolo C, Patanè S, et al. Transition metal oxides on reduced graphene oxide nanocomposites: Evaluation of physicochemical properties. J Nanomaterials. 2019;1-9.
- [174] Athira AR, Merin T, Anupama K, Mary KA, Xavier TS. Surfactant incorporated polyaniline/Co3O4/rGO ternary hybrid composite symmetric supercapacitors for efficient energy storage applications. Diam Relat Mater. 2022;130:109475.
- Elayappan V, Muthusamy S, Mayakrishnan G, Balasubramaniam R, Lee YS, Noh HS, et al. Ultrasonication-drybased synthesis of gold nanoparticle-supported CuFe on rGO nanosheets for competent detection of biological molecules. Appl Surf Sci. 2020;531:147415.
- [176] Acharya J, Pant B, Ojha GP, Park M. Embellishing hierarchical 3D core-shell nanosheet arrays of ZnFe2O4@ NiMoO4 onto rGO-Ni foam as a binder-free electrode for asymmetric supercapacitors with excellent electrochemical performance. | Colloid Interface Sci. 2022:610:863-78.
- [177] Ishaq S, Moussa M, Kanwal F, Ehsan M, Saleem M, Van TN, et al. Facile synthesis of ternary graphene nanocomposites with doped metal oxide and conductive polymers as electrode materials for high performance supercapacitors. Sci Rep. 2019;9(1):5974.
- [178] Penke YK, Sinha P, Yadav AK, Ramkumar J, Kar KK. Al3+-doped 3dtransitional metal (Mn/Cu) ferrite impregnated rGO for PEC water-splitting/supercapacitor electrode with oxygen vacancies and surface intercalation aspects. Compos Part B: Eng. 2020;202:108431.
- [179] Gupta M, Tyagi S, Kumari N. Electrochemical evaluation of highly stable Mn ferrite/PEDOT/rGO ternary nanocomposite for supercapacitor electrodes. J Mater Science: Mater Electron. 2022;33(10):7838-52.
- [180] Rani B, Sahu NK. Electrochemical properties of CoFe2O4 nanoparticles and its rGO composite for supercapacitor. Diam Relat Mater. 2020;108:107978.
- [181] Kamar EA, Qasim KF, Mousa MA. Supercapacitor and oxygen evolution reaction performances based on rGO and Mn2V2O7 nanomaterials. Electrochim Acta. 2022;430:141106.
- [182] Wang Z, Zhang X, Li Y, Liu Z, Hao Z. Synthesis of graphene-NiFe 2 O 4 nanocomposites and their electrochemical capacitive behavior. J Mater Chem A. 2013;1(21):6393-9.
- [183] Srivastava A, Gupta GK, Srivastava SKK, Srivastava M, Sagar P, Anwar S. High-performance electrode based on Nife₂o₄ nanoparticles architectured R-Go Nanosheets for supercapacitors. 2022;1-23. doi: 10.2139/ssrn.418417.

- [184] Liang J, Wei Y, Zhang J, Yao Y, He G, Tang B, et al. Scalable green method to fabricate magnetically separable NiFe2O4-reduced graphene oxide nanocomposites with enhanced photocatalytic performance driven by visible light. Ind & Eng Chem Res. 2018;57(12):4311-9.
- [185] Hareesh K, Shateesh B, Joshi RP, Dahiwale SS, Bhoraskar VN, Haram SK, et al. PEDOT: PSS wrapped NiFe2O4/rGO tertiary nanocomposite for the super-capacitor applications. Electrochim Acta. 2016;201:106-16.
- Li C, Wang X, Li S, Li Q, Xu J, Liu X, et al. Optimization of NiFe2O4/ [186] rGO composite electrode for lithium-ion batteries. Appl Surf Sci. 2017;416:308-17.
- Shen J, Li X, Huang W, Li N, Ye M. One-pot polyelectrolyte assisted hydrothermal synthesis of NiFe2O4-reduced graphene oxide nanocomposites with improved electrochemical and photocatalytic properties. J Mater Res. 2014;29(18):2211-9.
- Darabi R, Shabani-Nooshabadi M. NiFe2O4-rGO/ionic liquid modified carbon paste electrode: An amplified electrochemical sensitive sensor for determination of Sunset Yellow in the presence of Tartrazine and Allura Red. Food Chem. 2021:339:127841.
- [189] Tamilselvi R, Lekshmi GS, Padmanathan N, Selvaraj V, Bazaka O, Levchenko I, et al. NiFe2O4/rGO nanocomposites produced by soft bubble assembly for energy storage and environmental remediation. Renew Energy. 2022;181:1386-401.
- [190] Ensafi AA, Zandi-Atashbar N, Gorgabi-Khorzoughi M, Rezaei B. Nickel-ferrite oxide decorated on reduced graphene oxide, an efficient and selective electrochemical sensor for detection of furazolidone. IEEE Sens J. 2019;19(14):5396-403.
- [191] Liu C, Zhang T, Cao L, Luo K. High-capacity anode material for lithium-ion batteries with a core-shell NiFe2O4/reduced graphene oxide heterostructure. ACS Omega. 2021;6(39):25269-76.
- Ensafi AA, Talkhooncheh BM, Zandi-Atashbar N, Rezaei B. Electrochemical sensing of flutamide contained in plasma and urine matrices using NiFe2O4/rGO nanocomposite, as an efficient and selective electrocatalyst. Electroanalysis. 2020;32(8):1717-24.
- [193] Wu F, Wang X, Li M, Xu H. A high capacity NiFe2O4/rGO nanocomposites as superior anode materials for sodium-ion batteries. Ceram Int. 2016;42(15):16666-70.
- [194] Cai YZ, Cao WQ, Zhang YL, He P, Shu JC, Cao MS. Tailoring rGO-NiFe2O4 hybrids to tune transport of electrons and ions for supercapacitor electrodes. J Alloy Compd. 2019;811:152011.
- [195] Uddin ME, Kim NH, Kuila T, Lee SH, Hui D, Lee JH. Preparation of reduced graphene oxide-NiFe2O4 nanocomposites for the electrocatalytic oxidation of hydrazine. Compos Part B: Eng. 2015;79:649-59.
- [196] Zhang Y, Cao W, Cai Y, Shu J, Cao M. Rational design of NiFe 2 O 4-rGO by tuning the compositional chemistry and its enhanced performance for a Li-ion battery anode. Inorg Chem Front. 2019;6(4):961-8.
- Boychuk VM, Zapukhlyak RI, Abaszade RG, Kotsyubynsky VO, [197] Hodlevsky MA, Rachiy BI, et al. Solution combustion synthesized NiFe2O4/reduced graphene oxide composite nanomaterials: morphology and electrical conductivity. Phys Chem Solid State. 2022;23(4):815-24.
- [198] Kaur R, Kaur J, Kumar V, Tikoo KB, Rana S, Kaushik A, et al. Unfolding the electrocatalytic efficacy of highly conducting NiFe2O4-rGO nanocomposites on the road to rapid and sensitive detection of hazardous p-Nitrophenol. J Electroanalytical Chem. 2021;887:115161.

- [199] Hodlevska M, Kotsyubynsky V, Boychuk V, Budzulyak I, Rachiy B, Zapukhlyak R, et al. Hydrothermally synthesized NiFe2O4/rGO composites: structure, morphology and electrical conductivity. Appl Nanosci. 2023;7:1–11.
- [200] Askari MB, Salarizadeh P. Binary nickel ferrite oxide (NiFe2O4) nanoparticles coated on reduced graphene oxide as stable and high-performance asymmetric supercapacitor electrode material. Int | Hydrog Energy. 2020;45(51):27482–91.
- [201] Mary BCJ, Vijaya JJ, Saravanakumar B, Bououdina M, Kennedy LJ. NiFe2O4 and 2D-rGO decorated with NiFe2O4 nanoparticles as highly efficient electrodes for supercapacitors. Synth Met. 2022;291:117201.
- [202] Chu D, Li F, Song X, Ma H, Tan L, Pang H, et al. A novel dual-tasking hollow cube NiFe2O4-NiCo-LDH@ rGO hierarchical material for high preformance supercapacitor and glucose sensor. J Colloid Interface Sci. 2020;568:130–8.
- [203] Askari MB, Salarizadeh P, Beitollahi H, Tajik S, Eshghi A, Azizi S. Electro-oxidation of hydrazine on NiFe2O4-rGO as a high-performance nano-electrocatalyst in alkaline media. Mater Chem Phys. 2022;275:125313.
- [204] Samson VAF, Bernadsha SB, Britto JF, Raj MVA, Madhavan J. Synthesis of rGO/NiFe2O4 nanocomposite as an alternative counter electrode material to fabricate Pt-free efficient dye sensitized solar cells. Diam Relat Mater. 2022;130:109406.
- [205] Cai YZ, Cao WQ, He P, Zhang YL, Cao MS. NiFe2O4 nanoparticles on reduced graphene oxide for supercapacitor electrodes with improved capacitance. Mater Res Express. 2019;6(10):105535.
- [206] Zhang X, Zhu M, Ouyang T, Chen Y, Yan J, Zhu K, et al. NiFe2O4 nanocubes anchored on reduced graphene oxide cryogel to achieve a 1.8 V flexible solid-state symmetric supercapacitor. Chem Eng J. 2019;360:171–9.
- [207] Deyab MA, Awadallah AE, Ahmed HA, Mohsen Q. Progress study on nickel ferrite alloy-graphene nanosheets nanocomposites as supercapacitor electrodes. J Energy Storage. 2022;46:103926.
- [208] Chen J, Zhang F, Li Z, Ren X, Han S, Cai M, et al. 3D hierarchical NiFe2O4 nanosheets/Ni foam electrode using for high performance supercapacitor. Int J Electrochem Sci. 2022;17(9):1–11.
- [209] Pan J, Li S, Li F, Yu T, Liu Y, Zhang L, et al. The NiFe2O4/NiCo $_2O_4$ / GO composites electrode material derived from dual-MOF for high performance solid-state hybrid supercapacitors. Colloids Surf A: Physicochemical Eng Asp. 2021;609:125650.
- [210] Sivakumar M, Muthukutty B, Panomsuwan G, Veeramani V, Jiang Z, Maiyalagan T. Facile synthesis of NiFe2O4 nanoparticle with carbon nanotube composite electrodes for high-performance asymmetric supercapacitor. Colloids Surf A: Physicochemical Eng Asp. 2022;648:129188.
- [211] Patil PD, Shingte SR, Karade VC, Kim JH, Dongale TD, Mujawar SH, et al. Effect of annealing temperature on morphologies of metal organic framework derived NiFe2O4 for supercapacitor application. J Energy Storage. 2021;40:102821.
- [212] Iqbal Z, Tanweer MS, Alam M. Reduced graphene oxide-modified spinel cobalt ferrite nanocomposite: synthesis, characterization, and its superior adsorption performance for dyes and heavy metals. ACS Omega. 2023;8(7):6376–90.
- [213] Verma S, Das T, Pandey VK, Verma B. Nanoarchitectonics of GO/ PANI/CoFe2O4 (Graphene Oxide/polyaniline/Cobalt Ferrite) based hybrid composite and its use in fabricating symmetric supercapacitor devices. J Mol Structure. 2022;1266:133515.
- [214] Martinez-Vargas S, Mtz-Enriquez AI, Flores-Zuñiga H, Encinas A, Oliva J. Enhancing the capacitance and tailoring the discharge

- times of flexible graphene supercapacitors with cobalt ferrite nanoparticles. Synth Met. 2020;264:116384.
- [215] Gao L, Han E, He Y, Du C, Liu J, Yang X. Effect of different templating agents on cobalt ferrite (CoFe 2 O 4) nanomaterials for high-performance supercapacitor. Ionics. 2020;26:3643–54.
- [216] Alruwashid FS, Dar MA, Alharthi NH, Abdo HS. Effect of graphene concentration on the electrochemical properties of cobalt ferrite nanocomposite materials. Nanomaterials. 2021;11(10):2523.
- [217] Sidiqua MA, Priya VS, Begum N, Aman N. Synthesis of magnetic ZnFe2O4-reduced graphene oxide nanocomposite photocatalyst for the visible light degradation of cationic textile dyes.

 Nanotechnol Environ Eng. 2023;8:1–11.
- [218] Chen TW, Rajaji U, Chen SM, Al Mogren MM, Hochlaf M, Al Harbi SDA, et al. A novel nanocomposite with superior electrocatalytic activity: A magnetic property based ZnFe2O4 nanocubes embellished with reduced graphene oxide by facile ultrasonic approach. Ultrason Sonochem. 2019;57:116–24.
- [219] Ghasemi AK, Ghorbani M, Lashkenari MS, Nasiri N. Controllable synthesis of zinc ferrite nanostructure with tunable morphology on polyaniline nanocomposite for supercapacitor application. J Energy Storage. 2022;51:104579.
- [220] Askari MB, Salarizadeh P, Seifi M, Di Bartolomeo A. ZnFe2O4 nanorods on reduced graphene oxide as advanced supercapacitor electrodes. J Alloy Compd. 2021;860:158497.
- [221] Xu B, Yu L, Zhao X, Wang H, Wang C, Zhang LY, et al. Simple and effective synthesis of zinc ferrite nanoparticle immobilized by reduced graphene oxide as anode for lithium-ion batteries. J Colloid Interface Sci. 2021;584:827–37.
- [222] Lakra R, Mahender C, Singh BK, Kumar R, Kumar S, Sahoo PK, et al. ZnFe2O4 nanoparticles supported on graphene nanosheets for high-performance supercapacitor. J Electron Mater. 2023;52(4):2676–84.
- [223] Israr M, Iqbal J, Arshad A, Aisida SO, Ahmad I. A unique ZnFe2O4/ graphene nanoplatelets nanocomposite for electrochemical energy storage and efficient visible light driven catalysis for the degradation of organic noxious in wastewater. J Phys Chem Solids. 2020:140:109333.
- [224] Mary B, Vijaya JJ, Nair RR, Mustafa A, Selvamani PS, Saravanakumar B, et al. Reduced graphene oxide-tailored CuFe₂O₄ nanoparticles as an electrode material for high-performance supercapacitors. J Nanomater. 2022;2022(1):1–15. doi: 10. 1155/2022/9861440.
- [225] Israr M, Iqbal J, Arshad A, Sadaf A, Rani M, Rani M, et al. CuFe2O4/ GNPs nanocomposites for symmetric supercapacitors and photocatalytic applications. J Phys D: Appl Phys. 2021;54(39):395501.
- [226] Makkar P, Gogoi D, Roy D, Ghosh NN. Dual-purpose CuFe2O4rGO-based nanocomposite for asymmetric flexible supercapacitors and catalytic reduction of nitroaromatic derivatives. ACS Omega. 2021;6(43):28718–28.
- [227] Polat S, Faris D. Fabrication of CuFe2O4@ g-C3N4@ GNPs nanocomposites as anode material for supercapacitor applications. Ceram Int. 2022;48(17):24609–18.
- [228] Sohail Y, Liaquat A, Haq AU, Zafar MF, Ul-Haq N. Impedance spectroscopy and investigation of conduction mechanism in reduced graphene/CuFe 2 O 4 nanocomposites. Appl Phys A. 2021:127:1–10.
- [229] Astaraki H, Masoudpanah SM, Alamolhoda S. Effects of fuel contents on physicochemical properties and photocatalytic activity of CuFe₂O₄/reduced graphene oxide (rGO)

- nanocomposites synthesized by solution combustion method. J Mater Res Technol. 2020;9(6):13402-10.
- [230] Abdel-Salam AI, Attia SY, El-Hosiny FI, Sadek MA, Mohamed SG, Rashad MM. Facile one-step hydrothermal method for NiCo2S4/ rGO nanocomposite synthesis for efficient hybrid supercapacitor electrodes. Mater Chem Phys. 2022;277:125554.
- [231] Farshadnia M, Ensafi AA, Mousaabadi KZ, Rezaei B, Demir M. Facile synthesis of NiTe2-Co2Te2@ rGO nanocomposite for highperformance hybrid supercapacitor. Sci Rep. 2023;13(1):1364.
- [232] Askari MB, Salarizadeh P, Di Bartolomeo A, Şen F. Enhanced electrochemical performance of MnNi2O4/rGO nanocomposite as pseudocapacitor electrode material and methanol electrooxidation catalyst. Nanotechnology. 2021;32(32):325707.
- [233] Murugan E. Govindaraiu S. Santhoshkumar S. Hydrothermal synthesis, characterization and electrochemical behavior of NiMoO4 nanoflower and NiMoO4/rGO nanocomposite for high-performance supercapacitors. Electrochim Acta. 2021;392:138973.
- [234] Adib K, Sohouli E, Ghalkhani M, Naderi HR, Rezvani Z, Rahimi-Nasrabadi M. Sonochemical synthesis of Ag2WO4/rGO-based nanocomposite as a potential material for supercapacitors electrodes. Ceram Int. 2021;47(10):14075-86.
- Askari N, Salarizadeh N, Askari MB. Electrochemical determina-[235] tion of rutin by using NiFe2O4 nanoparticles-loaded reduced graphene oxide. J Mater Science: Mater Electron. 2021;32(8):9765-75.
- [236] Yao C, Su Y, Li Y, Li J. Preparation and electrochemical properties of NiCo2O4/rGO composites. Int J Electrochem Sci. 2021;16(1):150917.
- [237] Kumar GS, Reddy SA, Maseed H, Reddy NR. Facile hydrothermal synthesis of ternary CeO2-SnO2/rGO nanocomposite for supercapacitor application. Functional. Mater Lett. 2020;13(02):2051005.
- [238] Nihal A, Gulati P, Singh JP, Singh M, Kumar R, Singh H. Comparative analysis of tensile strength for corroded and uncorroded friction stir processed aluminum alloy surface composites. In: Jha K, Gulati P, Tripathi UK, editors. Recent advances in sustainable technologies. Lecture notes in mechanical engineering. Singapore: Springer; 2021. doi: 10.1007/978-981-16-0976-
- [239] Sharma H, Kumar K, Kumar R, Gulati P. A study of vibration and wear resistance of friction stir processed metal matrix composite. Mater Today: Proc. 2018;5(14):28354-63.
- [240] Sharma H, Tiwari SK, Chauhan VS, Kumar R, Gulati P. Wear analysis of friction stir processed aluminum composite reinforced by boron carbide. Mater Today: Proc. 2021;46(Part 6):2141-5. doi: 10. 1016/j.matpr.2021.02.468.
- [241] Gulati P, Shukla DK, Gupta A, Singh M, Kumar R, Singh JP. Microstructural analysis of friction stir welded Mg AZ31 alloy. Mater Today: Proc. 2020;26(Part 2):1145-50. doi: 10.1016/j.matpr.
- [242] Chawla KK, Saini N, Dhiman R. Investigation of Tribological Behavior of Stainless Steel 304 and Grey Cast Iron Rotating Against EN32 Steel Using Pin on Disc Apparatus. IOSR J Mech Civ Eng. 2013;9:18-22.
- [243] Liu T, Li L, Zhang L, Cheng B, You W, Yu J. 0D/2D (Fe0. 5Ni0. 5) S2/ rGO nanocomposite with enhanced supercapacitor and lithium ion battery performance. | Power Sources. 2019;426:266-74.
- [244] Choudhary RB, Kandulna R. 2-D rGO impregnated circular-tetragonal-bipyramidal structure of PPY-TiO2-rGO nanocomposite as

- ETL for OLED and supercapacitor electrode materials. Mater Sci Semiconductor Process. 2019;94:86-96.
- [245] Zhang X, Tang Y, Zhang F, Lee C. A novel aluminum-graphite dualion battery. Adv Energy Mater. 2016;6(11):1502588. doi: 10.1002/ aenm.201502588.
- [246] Wang M, Jiang C, Zhang S, Song X, Tang Y, Cheng H. Reversible calcium alloying enables a practical room-temperature rechargeable calcium-ion battery with a high discharge voltage. Nat Chem. 2018;10(6):667-72. doi: 10.1038/s41557-018-0045-4.
- [247] Yang J, Shang J, Liu Q, Yang X, Tan Y, Zhao Y, et al. Variantlocalized high-concentration electrolyte without phase separation for low-temperature batteries. Angew Chem Int Ed. 2024;63:e202406182. doi: 10.1002/anie.202406182.
- [248] Wang L, Lu J, Li S, Xi F, Tong Z, Chen X, et al. Controllable interface engineering for the preparation of high rate silicon anode. Adv Funct Mater. 2024;34:2403574. doi: 10.1002/adfm.202403574.
- [249] Liu Y, Liu X, Li X, Yuan H. Analytical model and safe-operation-area analysis of bridge-leg crosstalk of GaN E-HEMT considering correlation effect of multi-parameters. IEEE Trans Power Electron. 2024;39(7):8146-61. doi: 10.1109/TPEL.2024.3381638.
- [250] Zhou H, Su W, Xing Y, Wang J, Zhang W, Jia H, et al. Progress of catalytic oxidation of VOCs by manganese-based catalysts. Fuel. 2024;366:131305. doi: 10.1016/j.fuel.2024.131305.
- [251] Wang X, Luo Z, Huang J, Chen Z, Xiang T, Feng Z, et al. S/N-codoped graphite nanosheets exfoliated via three-roll milling for high-performance sodium/potassium ion batteries. J Mater Sci & Technol. 2023;147:47-55. doi: 10.1016/j.jmst.2022.11.015.
- [252] Wang X, Xia Y, Huang J, Su Y, Chen Z, Chen L, et al. A facile strategy for large-scale production of 2D nanosheets exfoliated by threeroll milling. J Adv Ceram. 2024;13(1):11-8. doi: 10.26599/JAC.2024. 9220831.
- [253] Mohammed KA, AlKareem Shihab SA, Algburi S, Bhavani B, Kareem A, Alkhafaji MA, et al. Synthesis and characterization of PVA-encapsulated Fe2O3-ZnO as new composites with tunable optical properties. Rev des Compos et des Matériaux Avancés. 2024;34:1099-106. doi: 10.18280/rcma.340205.
- [254] Mohammed KA, Al-alawachi SF, Hassan AA, Alkhayatt AH, Abood MM, Alkhafaji MA, et al. The Impact of polymer matrix type on the optical properties of silver nanocomposites. E3S Web Conf. 2024:505:1017. doi: 10.1051/e3sconf/202450501017.
- [255] Jarad AN, Abed AS, Mohammed KA, Zabibah RS, Al-khafaji M, Algburi S, et al. Preparing and studying of Au Nanocomposites Synthesized with different polymer matrix. E3S Web Conf. 2024;505:01035. doi: 10.1051/e3sconf/202450501035.
- [256] Mohammed KA, Talib RA, Algburi S, Kareem A, Bhavani B, Alkhafaji MA, et al. Synthesis PEO/PS/PMMA/Se as new nanocomposite with porous morphology. Chalcogenide Lett. 2023;20:863-70. doi: 10.15251/CL.2023.2012.863.
- [257] Sharma S, Sudhakara P, Singh J, Siengchin S. Fabrication of novel polymer composites from leather waste fibers and recycled poly (ethylene-vinyl-acetate) for value added products. Sustainability. 2023;15(5):4333. doi: 10.3390/su15054333.
- [258] Sharma S, Sudhakara P, Petru M, Singh J, Rajkumar S. Effect of nanoadditives on the novel leather fiber/recycled poly(ethylenevinyl-acetate) polymer composites for multifunctional applications: fabrication, characterizations, and multiobjective optimization using central composite design. Nanotechnol Rev. 2022;11(1):2366e432. doi: 10.1515/ntrev-2022-0067.
- [259] Mohammed KA, Salem KH, Jawaad MF, Alkhafaji MA, Zabibah RS. Designing and studying of PVA/Fe2O3/Se as new ovonic material

36

- for possible storage application. J Ovonic Res. 2023;19:615–22. doi: 10.15251/JOR.2023.196.615.
- [260] Sharma S, Sudhakara P, Singh J, Singh S, Singh G. Emerging progressive developments in the fibrous composites for acoustic applications. J Manuf Process. 2023;102:443e77. doi: 10.1016/j. jmapro.2023.07.053.
- [261] Mohammed KA, Abdul Kareem AAH, Judi HK, Rathan A, Algburi S, Alkhafaji MA, et al. Synthesis and examination of new PVA-Fe₂O₃-Au hybrid composite. Iranian. J Phys Res. 2023;23(3):135–9.
- [262] Yeswanth IVS, Kanishka J, Shantanu BR, Kumar R, Sharma S, Ilyas RA. Recent developments in RAM based MWCNT composite materials: a short review. Funct Compos Struct. 2022;42:024001.
- [263] Jain A, Nabeel AN, Bhagwat S, Kumar R, Sharma S, Kozak D, et al. Fabrication of polypyrrole gas sensor for detection of NH3 using an oxidizing agent and pyrrole combinations: Studies and characterizations. Heliyon. 2023 Jun;9(7):e17611. doi: 10.1016/j.heliyon. 2023.e17611. PMID: 37455973; PMCID: PMC10338976.
- [264] Sharma S, Sudhakara P, Borhana A, Singh J, Ilyas RA. Recent trends and developments in Conducting Polymer Nanocomposites for Multifunctional applications. Polymers. 2021;13(17):2898. doi: 10.3390/polym13172898.
- [265] Sharma S, Verma A, Rangappa SM, Siengchin S, Ogata S. Recent progressive developments in conductive-fillers based polymer nanocomposites (CFPNC's) and conducting polymeric nanocomposites (CPNC's) for multifaceted sensing applications. J Mater Res Technol. S2238–7854(23):02112–9. doi: 10.1016/j.jmrt.2023.08.300.